Reliability analysis and updating of deteriorating systems with subset simulation

Ronald Schneider[1,*], Sebastian Thöns[2] and Daniel Straub[3]

[1]Bundesanstalt für Materialforschung und -prüfung (BAM), 7. Safety of Structures, Unter den Eichen 87, 12205 Berlin, Germany

[2]Technical University of Denmark (DTU), Department of Civil Engineering, Brovej, 2800 Kongens Lyngby, Denmark

[3]Technische Universität München (TUM), Engineering Risk Analysis Group, Arcisstr. 21, 80290 Munich, Germany

*Corresponding author: Tel.: +49-30-8104 4372 Email: ronald.schneider@bam.de

Abstract

An efficient approach to reliability analysis of deteriorating structural systems is presented, which considers stochastic dependence among element deterioration. Information on a deteriorating structure obtained through inspection or monitoring is included in the reliability assessment through Bayesian updating of the system deterioration model. The updated system reliability is then obtained through coupling the updated deterioration model with a probabilistic structural model. The underlying high-dimensional structural reliability problems are solved using subset simulation, which is an efficient and robust sampling-based algorithm suitable for such analyses. The approach is demonstrated in two case studies considering a steel frame structure and a Daniels system subjected to high-cycle fatigue.

Keywords

Structural reliability, deterioration, Bayesian analysis, inspection, monitoring, subset simulation

1 Introduction

Engineering structures are generally subjected to deterioration processes such as fatigue and corrosion, and their structural reliability may thus reduce over time. Predictions of the deterioration progress with quantitative models are uncertain due to the simplified representation of the actual deterioration phenomena, the inherent variability of the influencing parameters and limited information on those parameters. These uncertainties must be addressed when modeling

34　deterioration of structures (Lin and Yang 1985; Madsen et al. 1986; Melchers 1999a). Inspections

35　and monitoring are effective means of obtaining information on the actual condition of

36　deteriorating structures. This information should be utilized to reduce uncertainties in probabilistic

37　models. A consistent framework for this task is provided by Bayesian analysis, in which prior

38　probabilistic models are updated with inspection and monitoring outcomes (e.g. Tang 1973;

39　Madsen 1987; Enright and Frangopol 1999). This approach facilitates the quantification of the

40　effect of inspection and monitoring results on the structural reliability, and forms the basis for

41　decisions on maintenance actions and future inspection efforts (e.g. Thoft-Christensen and

42　Sørensen 1987; Faber et al. 2000; Moan 2005; Straub and Faber 2005).

43　Deterioration processes are generally correlated among structural elements within a system due to

44　common influencing factors, such as environmental conditions and material characteristics (e.g.

45　Moan and Song 2000; Vrouwenvelder 2004; Straub and Faber 2005; Stewart and Mullard 2007).

46　This leads to a correlation among deterioration failures of different elements whose effect on the

47　system reliability has to be assessed as a function of structural redundancy (Straub and Der

48　Kiureghian 2011). Correlation among element deterioration is especially relevant when inspection

49　and monitoring outcomes are considered in the reliability assessment (Vrouwenvelder 2004). An

50　observation at one location within a structure contains more indirect information on the

51　deterioration progress at another location if the correlation among element deterioration is high.

52　For these reasons, the reliability of deteriorating structures should be analyzed and updated

53　considering the structure as a whole.

54　A number of publications propose methods for computing the time-variant reliability of

55　deteriorating structures, including works by Mori and Ellingwood (1993), Li (1995), Ciampoli

56　(1998), Estes and Frangopol (1999), Stewart and Val (1999) and Li et al. (2015). They consider

57　the time-dependent characteristics of both the load and resistance, but do not account for

58　correlation among element deterioration. More recently, a number of researchers have considered

59　modeling and updating the system deterioration state of structures, taking into account the aspect

60　of spatial correlation among element deterioration (Moan and Song 2000; Li et al. 2004; Faber et

61　al. 2006; Straub 2011b; Qin and Faber 2012; Maljaars and Vrouwenvelder 2014). Therein, the

62　effect of inspections and monitoring results on the probability of either reinforcement corrosion in

63　concrete structures or fatigue failures in steel structures is quantified using Bayesian analysis.

64　However, the impact of deterioration on the structural reliability is not included in these works.

65　Such integrated system reliability analyses are proposed in (Lee and Song 2014; Schneider et al.

66　2015; Luque and Straub 2016). Lee and Song (2014) consider sequential fatigue failures taking

67　into account the effect of stress redistribution within a structural system. They identify critical

68　failure sequences through a branch-and-bound scheme and iteratively compute and update bounds

69　on the system failure probability. Luque and Straub (2016) and Schneider et al. (2015) propose the

70　use of hierarchical Dynamic Bayesian Network (DBN) models for probabilistically representing

71　deterioration in structural systems and for updating deterioration probabilities as well as the system

72 reliability with inspection and monitoring results. While they can be powerful, DBN models are
73 rather demanding in the implementation.

74 To enable an integrated system reliability analysis of inspected and monitored deteriorating
75 structures, which is computationally efficient and simple to implement, we here develop a
76 framework using two coupled sub-models: a probabilistic system deterioration model, which
77 considers stochastic dependence among element deterioration, and a probabilistic structural model
78 for calculating the failure probability of the weakened system. Motivated by the work of Straub
79 and Der Kiureghian (2011), the system deterioration state is assessed at discrete time intervals and
80 is considered constant within each interval. Information on the deteriorating structure obtained
81 through inspection or monitoring is included in the reliability assessment through Bayesian
82 updating of the system deterioration model. The updated system reliability is then obtained through
83 coupling this updated model with a probabilistic structural model. The resulting structural
84 reliability problems are high-dimensional since they include all (correlated) deteriorating
85 elements. To solve these problems, we apply subset simulation, which is a sampling-based
86 algorithm that can robustly and efficiently handle problems involving a large number of random
87 variables. The method is demonstrated in two case studies considering welded steel structures
88 subjected to fatigue deterioration.

2   System reliability analysis of deteriorating structures

2.1   Deterioration modeling

91 Deterioration is modeled at the element level at discrete time steps. An element may be a structural
92 member, a welded connection or a segment of a continuous surface (Straub and Der Kiureghian
93 2011). The state of deterioration of an element i at time t is represented by a random variable or
94 random vector $D_{i,t}$. For example, in the context of reinforcement corrosion in concrete structures,
95 $D_{i,t}$ may represent the loss of reinforcement cross section. Deterioration of all elements is
96 influenced by a set random variables $\mathbf{X} = (X_1, \dots, X_n)$. The relationship between $\mathbf{X}$ and $D_{i,t}$ is
97 described by a parametric deterioration model h_i, which is written in generic form as:

$$D_{i,t} = h_i(\mathbf{X}, t) \tag{1}$$

98 The joint probability density function (PDF) of $\mathbf{X}$ is denoted by $f_{\mathbf{X}}(\mathbf{x})$. Model uncertainties arising
99 from a simplified representation of the actual deterioration phenomenon are included through
100 additional random variables in $\mathbf{X}$.

101 All random variables describing the deterioration state of the individual elements at time t are
102 summarized in a vector $\mathbf{D}_t = (D_{1,t}, \dots, D_{n_E,t})$, where n_E is the number of elements considered in
103 the system reliability analysis. This vector represents the overall deterioration state of the structural

104 system at time t. The relationship between the system deterioration state $\mathbf{D}_t$ and the deterioration
105 model parameter $\mathbf{X}$ is described by a function $\mathbf{h}$ as:

$$\mathbf{D}_t = \mathbf{h}(\mathbf{X}, t) = \left(h_1(\mathbf{X}, t), \dots, h_{n_E}(\mathbf{X}, t) \right) \tag{2}$$

106   2.2   Modeling dependence among deterioration model parameters

107 Deterioration of different elements of a structural system is generally interdependent due to the
108 spatial correlation among the uncertain parameters $\mathbf{X}$ influencing their condition. Such spatial
109 dependencies are often due to geometrical proximity, but they mainly exist due to common factors
110 influencing the element condition such as environmental conditions and material characteristics
111 (Luque and Straub 2016). The aspect of spatial correlation of deterioration is especially relevant
112 when inspection and monitoring outcomes are considered in the reliability assessment of
113 deteriorating structures. The effect of such observations on the reliability strongly depends on the
114 spatial correlation among the parameters $\mathbf{X}$. An observation at one location contains more indirect
115 information on the deterioration progress at another location if the correlation among the
116 parameters $\mathbf{X}$ is high.

117 There is only limited information available on modeling statistical dependence of deterioration in
118 structural systems (e.g. Vrouwenvelder 2004; Malioka 2009; Luque et al. 2016). For example,
119 Vrouwenvelder (2004) estimated the correlation among uncertain parameters influencing fatigue
120 crack growth in welded connections by comparing the scatter of the parameters within one
121 production series to the scatter in the overall population. In most applications, however, correlation
122 among the uncertain parameters $\mathbf{X}$ has to be estimated based at least partially on engineering
123 judgment.

124 Hierarchical models and random field models are commonly applied to represent spatial
125 dependence among the uncertain parameters $\mathbf{X}$. The latter are suitable for representing parameters
126 with inherent spatial variability (e.g. Hergenröder 1992; Stewart and Mullard 2007; Malioka
127 2009). The random field approach models a spatially varying parameter X as a random variable
128 $X(z)$ at each location z, and describes the correlation structure of the different random variables
129 $X(z)$ in terms of a suitable correlation function. Such random fields are typically discretized to
130 enable their numerical representation (see, for example, Betz et al. 2014a). As a result, a random
131 field of a spatially varying parameter is defined by a discrete set of correlated random variables,
132 which are part of $\mathbf{X}$. The joint distribution of the variables in a random field is commonly
133 represented by the Nataf model, also known as the Gaussian copula (Liu and Der Kiureghian
134 1986).

135 Hierarchical models may be applied if common influencing factors can be modeled explicitly (e.g.
136 Maes and Dann 2007; Luque et al. 2016). Such models represent correlation among random
137 variables by defining different levels. The random variables within one level are linked through

138 common influencing factors, which are modeled as random variables at a higher level in the
139 hierarchy. The random variables at the highest level are often called hyper-parameters (see, for
140 example, Maes and Dann 2007). The additional random variables representing common influencing
141 factors in a hierarchical model are included in **X**. The probability distributions of the random
142 variables in each level are defined conditional on the random variables at the next higher level in
143 the hierarchy. Such a hierarchical dependence structure among the variables in **X** can be
144 implemented through the Rosenblatt transformation (Hohenbichler and Rackwitz 1981).

145 In many instances common influencing factors can, however, not be modeled explicitly. Instead,
146 statistical dependence among the variables in **X** is often represented by correlation coefficients. As
147 an example, statistical dependence of fatigue deterioration among welded connections due to
148 common fabrication quality may be modeled by defining a correlation coefficient between the
149 initial crack sizes at different hotspots (Vrouwenvelder 2004). In this case, the Nataf model can be
150 applied to model the joint distribution of the correlated deterioration model parameters.

151 Parameters influencing deterioration can also be time variant. Such parameters are ideally modeled
152 by stochastic processes (see, for example, Lin and Yang 1985; Straub and Faber 2007; Altamura
153 and Straub 2014). Similar to a random field, a stochastic process represents a time-varying
154 parameter X as a random variable $X(t)$ at each time t, and describes the correlation among the
155 random variables $X(t)$ through a suitable correlation function. Continuous-time stochastic
156 processes are discretized to facilitate their numerical representation. The resulting set of correlated
157 random variables is included in **X**. The joint distribution of the variables in a stochastic process
158 may be represented by the Nataf model. In case a stochastic process has the Markov property, the
159 Rosenblatt transformation may be applied (see, for example, Altamura and Straub 2014).

2.3 Prior system failure probability

161 The system failure probability is assessed conditional on the system deterioration state $\mathbf{D}_t$. In
162 agreement with Straub and Der Kiureghian (2011), the deterioration state of a structure is
163 considered constant over a period Δt. The value of Δt depends on how fast deterioration progresses
164 and on the lifetime of the structure. In most applications, a good choice is $\Delta t = 1$ year, which is
165 short compared to the typical lifetime of structural systems. Conservatively, the system
166 deterioration state in the period $[t - \Delta t, t]$ is set equal to the state at time t, $\mathbf{D}_t$. The relationship
167 between the system deterioration state $\mathbf{D}_t$ and the deterioration model parameters **X** is described
168 by Equation (2). Let F_t denote the event of system failure in the period $[t - \Delta t, t]$. The probability
169 of this event conditional on a realization of the deterioration model parameters **x** is written as:

$$p_F(\mathbf{x}, t) = \Pr(F_t|\mathbf{X} = \mathbf{x}) = \Pr\big(F_t|\mathbf{D}_t = \mathbf{h}(\mathbf{x}, t)\big) \tag{3}$$

170 To include the uncertainty in the deterioration model parameters, the total probability theorem is
171 applied. The overall probability of system failure in the reference period $[t - \Delta t, t]$ is:

$$\Pr(F_t) = \int_{D_{\mathbf{X}}} \Pr(F_t|\mathbf{X} = \mathbf{x}) f_{\mathbf{X}}(\mathbf{x}) \, d\mathbf{x} = \int_{D_{\mathbf{X}}} p_F(\mathbf{x}, t) f_{\mathbf{X}}(\mathbf{x}) \, d\mathbf{x} \tag{4}$$

172   where $D_{\mathbf{X}}$ denotes the domain of definition of $\mathbf{X}$. The total-probability-form of the structural
173   reliability problem is advantageous when random variables not contained in $\mathbf{X}$ also influence the
174   event of system failure F_t (Straub and Der Kiureghian 2010). Such random variables are
175   considered in the computation of $p_F(\mathbf{x}, t)$. By defining the problem in this form, the deterioration
176   model is decoupled from the structural model.

177   The conditional system failure probability $p_F(\mathbf{x}, t) = \Pr\big(F_t|\mathbf{D}_t = \mathbf{h}(\mathbf{x}, t)\big)$ is computed by
178   performing system reliability analyses of the damaged structure. To this end, the structural model
179   is defined with element properties according to the system deterioration state $\mathbf{D}_t = \mathbf{h}(\mathbf{x}, t)$.
180   Random variables influencing the system reliability which are not contained in $\mathbf{X}$ are typically load
181   and resistance parameters. While resistance parameters, such as material strengths and structural
182   dimensions, are usually modeled as time-invariant random variables, load parameters are mostly
183   stochastic processes. However, it is typically sufficient to represent the load process by its extreme
184   value distribution for the reference period $[t - \Delta t, t]$ (Melchers 1999b; Straub and Der Kiureghian
185   2011). The computation of $p_F(\mathbf{x}, t)$ then reduces to a time-invariant reliability analysis of the
186   weakened system. This approach leads to an accurate solution if the load process is ergodic and
187   the maximum loads in two different time periods are statistically independent of each other. This
188   holds at least approximately for most relevant applications.

189   Equation (4) can be transformed into a component reliability problem following Wen and Chen
190   (1987). To this end, we introduce an auxiliary standard uniform random variable P with PDF
191    $f_P(p) = 1$ and cumulative distribution function (CDF) $F_P(p) = p$. We now note that the following
192   identity holds:

$$p_F(\mathbf{x}, t) = F_P\big(p_F(\mathbf{x}, t)\big) = \Pr\big(P \le p_F(\mathbf{x}, t)\big) \tag{5}$$

193   The right hand side of Equation (5) corresponds to a component reliability problem with limit-
194   state function:

$$g_F(\mathbf{x}, p, t) = p - p_F(\mathbf{x}, t) \tag{6}$$

195   The limit-state function $g_F(\mathbf{x}, p, t)$ describes a domain $\Omega_F(t)$ in the augmented outcome space of
196    $\mathbf{X}$ and P as $\Omega_F(t) = \{(\mathbf{x}, p) : g_F(\mathbf{x}, p, t) \le 0\}$. The conditional probability $p_F(\mathbf{x}, t)$ can now be
197   expressed as:

$$p_F(\mathbf{x}, t) = \int_{p \in \Omega_F(t)} f_P(p) \, dp = \int_0^1 I(g_F(\mathbf{x}, p, t) \le 0) f_P(p) \, dp \tag{7}$$

198   where $I(\cdot)$ is the indicator function: $I(\cdot) = 1$ if the condition $(\cdot)$ is true and $I(\cdot) = 0$ otherwise.

199   Inserting Equation (7) into Equation (4) gives:

$$
\begin{aligned}
\Pr(F_t) &= \int_{D_\mathbf{X}} \left[\int_0^1 I(g_F(\mathbf{x}, p, t) \leq 0)\, f_P(p)\, dp \right] f_\mathbf{X}(\mathbf{x})\, d\mathbf{x} \\
&= \int_{D_\mathbf{X}} \int_0^1 I(g_F(\mathbf{x}, p, t) \leq 0)\, f_\mathbf{X}(\mathbf{x})\, f_P(p)\, d\mathbf{x}\, dp \\
&= \int_{(\mathbf{x}, p) \in \Omega_F(t)} f_\mathbf{X}(\mathbf{x})\, f_P(p)\, d\mathbf{x}\, dp
\end{aligned}
\tag{8}
$$

200   Equation (8) can be solved using structural reliability methods (e.g. Ditlevsen and Madsen 1996).
201   As discussed earlier, such a calculation requires the computation of the conditional system failure
202   probability $p_F(\mathbf{x}, t) = \Pr\big(F_t | \mathbf{D}_t = \mathbf{h}(\mathbf{x}, t)\big)$, which can be determined using system reliability
203   analysis methods (see, for example, Hohenbichler and Rackwitz 1983; Ditlevsen and Bjerager
204   1986; Thoft-Christensen and Murotsu 1986; Naess et al. 2009; Song and Kang 2009). If the
205   number of distinct system deterioration states $\mathbf{D}_t = \mathbf{d}_t$ is limited, $\Pr(F_t | \mathbf{D}_t = \mathbf{d}_t)$ may be pre-
206   computed for all $\mathbf{D}_t = \mathbf{d}_t$. If this is not possible, $\Pr(F_t | \mathbf{D}_t = \mathbf{d}_t)$ has to be computed during the
207   evaluation of Equation (8). The computation of $\Pr(F_t | \mathbf{D}_t = \mathbf{d}_t)$ is discussed in more detail in
208   Section 7.

209   For the purpose of applying structural reliability methods, it is convenient to transform the
210   reliability problem defined in Equation (8) to standard normal space. To this end, the auxiliary
211   random variable P and the deterioration model parameters $\mathbf{X}$ are transformed to independent
212   standard normal random variables $\mathbf{U} = (U_0, U_1, \dots, U_n)$. P and $\mathbf{X}$ are independent and can be
213   transformed separately. The inverse transformation from $\mathbf{U}$ to P and $\mathbf{X}$ is as follows (see also Straub
214   and Papaioannou 2015b):

$$
P = \Phi(U_0) \tag{9}
$$

215   where $\Phi(\cdot)$ is the standard normal CDF, and

$$
\mathbf{X} = \mathbf{T}^{-1}(U_1, \dots, U_n) \tag{10}
$$

216      $\mathbf{T}(\cdot)$ is a probability preserving one-to-one mapping from the original outcome space of $\mathbf{X}$ to the
217   standard normal space for which the Rosenblatt transformation (Hohenbichler and Rackwitz 1981)
218   or the Nataf transformation (Liu and Der Kiureghian 1986) can be applied (see also Section 2.2).

219   The limit-state function g_F is now transformed to $\mathbf{U}$-space as:

$$
G_F(\mathbf{u}, t) = u_0 - \Phi^{-1}\big(p_F(\mathbf{T}^{-1}(u_1, \dots, u_n), t)\big) \tag{11}
$$

G_F describes the domain $\Omega_F^U(t)$ in the transformed space as $\Omega_F^U(t) = \{\mathbf{u} : G_F(\mathbf{u}, t) \leq 0\}$. Therefore, the system failure probability $\Pr(F_t)$ can be expressed in **U**-space as:

$$\Pr(F_t) = \Pr(G_F(\mathbf{U}, t) \leq 0) = \int_{\mathbf{u} \in \Omega_F^U(t)} \varphi_{n+1}(\mathbf{u}) \, d\mathbf{u} \tag{12}$$

where $\varphi_{n+1}(\mathbf{u}) = \prod_{i=0}^{n} \varphi(u_i)$ is the $(n+1)$-variate standard normal PDF and $\varphi(\cdot)$ is the standard normal PDF.

3 System reliability updating of deteriorating structures

3.1 Modeling observations with likelihood functions

In the context of deteriorating structures, inspections and monitoring systems typically provide direct or indirect information on the uncertain deterioration model parameters **X**. This information is usually imperfect due to measurement uncertainties and random errors. Generally, parameters influencing the deterioration process, the deterioration state of the structure itself, and quantities indirectly related to the deterioration state of the structure can be observed. Examples of such observations are results from half-cell potential measurements that provide indirect information on corrosion initiation in reinforced concrete structures and measurements of fatigue cracks in welded steel structures.

Mathematically, an inspection or monitoring outcome i at time t is an event, which is denoted by $Z_i(t)$ in the following. The relationship between $Z_i(t)$ and the uncertain deterioration model parameters **X** is modeled through a likelihood function $L_i(\mathbf{x}, t)$, which is proportional to the conditional probability of observing $Z_i(t)$ when the uncertain parameters **X** take a value **x**:

$$L_i(\mathbf{x}, t) \propto \Pr(Z_i(t) | \mathbf{X} = \mathbf{x}) \tag{13}$$

Generally, two types of observations can be distinguished: observations providing equality information and observations providing inequality information (Madsen et al. 1986; Straub 2011a). Observations providing equality information are observations that can be described by an observation event such as $Z_i(t) = \{y_i(t) = q_i(\mathbf{X}, t) + E_i\}$, where $y_i(t)$ is a measurement of a continuous quantity predicted by the model $q_i(\mathbf{X}, t)$ and E_i is an additive measurement error with PDF $f_{E_i}(\epsilon_i)$. The following equality holds $Y_i(t) - q_i(\mathbf{X}, t) = E_i$, where $Y_i(t)$ is the uncertain measurement outcome. In this special but common case, the likelihood of observing $Y_i(t) = y_i(t)$ given $\mathbf{X} = \mathbf{x}$ is equal to the probability density of the random measurement error E_i taking the value $y_i(t) - q_i(\mathbf{x}, t)$. The corresponding likelihood function can be written as (Straub and Papaioannou 2015b):

$$L_i(\mathbf{x}, t) = f_{E_i}\big(y_i(t) - q_i(\mathbf{x}, t)\big) \tag{14}$$

In the general case, the likelihood function of an observation $Z_i(t)$ of the equality-type is defined as (Straub and Papaioannou 2015b):

$$L_i(\mathbf{x}.t) = f_{Y_i(t)|\mathbf{X}}(y_i(t)|\mathbf{x}) \tag{15}$$

where $f_{Y_i(t)|\mathbf{X}}(y_i(t)|\mathbf{x})$ is the conditional PDF of the uncertain measurement outcome $Y_i(t)$ given $\mathbf{X} = \mathbf{x}$, which is typically defined in terms of the PDF of the associated measurement error E_i. The likelihood function defined in Equation (15) includes the evaluation of the model predicting the measured quantity as in Equation (14).

Observations providing inequality information are observations such as "corrosion progress is larger than a limit" or "no fatigue crack detected". An observation $Z_i(t)$ of the inequality type is modeled through a function $q_i(\mathbf{X}, t)$ as follows (Madsen et al. 1986):

$$Z_i(t) = \{q_i(\mathbf{X}, t) \le 0\} \tag{16}$$

A function $q_i(\mathbf{X}, t)$ of this type can be interpreted as a limit-state function. The corresponding likelihood function is written as (Straub and Papaioannou 2015b):

$$L_i(\mathbf{x}, t) = \Pr(Z_i(t)|\mathbf{X} = \mathbf{x}) = I(q_i(\mathbf{x}, t) \le 0) \tag{17}$$

The value of such a likelihood function is either 0 or 1.

All observations obtained in the period $[0, t]$ are expressed by a combined event $Z_{0:t}$ as follows:

$$Z_{0:t} = \bigcap_{j=1}^{n_Z(t)} \left(\bigcap_{i \in S_j} Z_i(t_j) \right) \tag{18}$$

where $n_Z(t)$ is the number of times at which inspections or measurements are performed in the period $[0, t]$ and S_j is an index set containing the indices of all observations at time t_j. The likelihood function describing the relationship between $Z_{0:t}$ and the uncertain deterioration model parameters $\mathbf{X}$ is defined as:

$$L(\mathbf{x}, t) \propto \Pr(Z_{0:t}|\mathbf{X} = \mathbf{x}) \tag{19}$$

Under the common assumption that all individual observations are statistically independent given the deterioration model parameters $\mathbf{X} = \mathbf{x}$, $L(\mathbf{x}, t)$ is computed as:

$$L(\mathbf{x}, t) = \prod_{j=1}^{n_Z(t)} \left(\prod_{i \in S_j} L_i(\mathbf{x}, t_j) \right) \tag{20}$$

267 In the case of statistically dependent observations, the combined likelihood has to be formulated
268 as a function of the joint distribution of all measurement errors. Straub and Papaioannou (2015a)
269 provide further details on how to model observations with likelihood functions.

3.2 Posterior system failure probability

271 The goal here is to assess the effect of inspection and monitoring outcomes on the failure
272 probability of deteriorating structural systems. In Bayesian analysis, this is achieved by computing
273 the conditional probability of the failure event F_t given the observation event $Z_{0:t}$, which is defined
274 as follows:

$$\Pr(F_t|Z_{0:t}) = \frac{\Pr(F_t \cap Z_{0:t})}{\Pr(Z_{0:t})} \tag{21}$$

275 We make the fundamental assumption that the system failure event F_t and the observation event
276 $Z_{0:t}$ are conditionally independent given the deterioration model parameters $\mathbf{X} = \mathbf{x}$. The joint
277 probability of the events F_t and $Z_{0:t}$ can therefore be written as:

$$\Pr(F_t \cap Z_{0:t}) = \int_{D_\mathbf{X}} \Pr(F_t|\mathbf{X} = \mathbf{x}) \Pr(Z_{0:t}|\mathbf{X} = \mathbf{x}) f_\mathbf{X}(\mathbf{x}) \, d\mathbf{x} \tag{22}$$

278 The probability of the observation outcome event can also be expressed in the total-probability-
279 form:

$$\Pr(Z_{0:t}) = \int_{D_\mathbf{X}} \Pr(Z_{0:t}|\mathbf{X} = \mathbf{x}) f_\mathbf{X}(\mathbf{x}) \, d\mathbf{x} \tag{23}$$

280 Following Straub (2011a), the integrals in Equations (22) and (23) are transformed such that they
281 can be solved using structural reliability methods. This method follows the same principles as
282 presented in Section 2.3 for the computation of $\Pr(F_t)$.

283 For the purpose of transforming Equations (23), an auxiliary standard normal random variable P
284 is again introduced. In addition, let c be a positive constant that ensures $0 \leq cL(\mathbf{x}, t) \leq 1$ for all
285 $\mathbf{x}$. In this case, the following relationship holds:

$$cL(\mathbf{x}, t) = F_P\big(cL(\mathbf{x}, t)\big) = \Pr\big(P \leq cL(\mathbf{x}, t)\big) \tag{24}$$

286 The right hand side of Equation (24) corresponds to a component reliability problem with limit-
287 state function:

$$g_{Z_e}(\mathbf{x}, p, t) = p - cL(\mathbf{x}, t) \tag{25}$$

288 The limit-state function $g_{Z_e}(\mathbf{x}, p, t)$ defines a domain $\Omega_{Z_e}(t)$ in the augmented outcome space of
289 $\mathbf{X}$ and P as $\Omega_{Z_e}(t) = \{(\mathbf{x}, p) : g_{Z_e}(\mathbf{x}, p, t) \leq 0\}$. The quantity $cL(\mathbf{x}, t)$ can be interpreted as the

290 conditional probability of P taking a value in $\Omega_{Z_e}(t)$ given $\mathbf{X} = \mathbf{x}$. It can thus be computed by
291 integrating $f_P(p)$ over the failure domain $\Omega_{Z_e}(t)$ when $\mathbf{X}$ take a value $\mathbf{x}$:

$$cL(\mathbf{x}, t) = \int_{p \in \Omega_{Z_e}(t)} f_P(p) \, dp = \int_0^1 I\big(g_{Z_e}(\mathbf{x}, p, t) \leq 0\big) f_P(p) \, dp \tag{26}$$

292 Consequently, the likelihood function $L(\mathbf{x}, t)$ can be written as:

$$L(\mathbf{x}, t) = \frac{1}{c} \int_0^1 I\big(g_{Z_e}(\mathbf{x}, p, t) \leq 0\big) f_P(p) \, dp \tag{27}$$

293 Let a denote the proportionality constant in the likelihood definition given in Equation (19). It
294 follows that:

$$\Pr(Z_{0:t} | \mathbf{X} = \mathbf{x}) = aL(\mathbf{x}, t) = \frac{a}{c} \int_0^1 I\big(g_{Z_e}(\mathbf{x}, p, t) \leq 0\big) f_P(p) \, dp \tag{28}$$

295 Inserting Equation (28) into Equation (23) gives:

$$\begin{aligned} \Pr(Z_{0:t}) &= \frac{a}{c} \int_{\mathbf{D_X}} \left[\int_0^1 I\big(g_{Z_e}(\mathbf{x}, p, t) \leq 0\big) f_P(p) \, dp \right] f_{\mathbf{X}}(\mathbf{x}) \, d\mathbf{x} \\ &= \frac{a}{c} \int_{(\mathbf{x}, p) \in \Omega_{Z_e}(t)} f_{\mathbf{X}}(\mathbf{x}) f_P(p) \, d\mathbf{x} \, dp \end{aligned} \tag{29}$$

296 Similarly, it can be shown that the probability of the joint event $F_t \cap Z_{0:t}$ can be written as:

$$\Pr(F_t \cap Z_{0:t}) = \frac{a}{c} \int_{(\mathbf{x}, p) \in \Omega_{F \cap Z_e}(t)} f_{\mathbf{X}}(\mathbf{x}) f_P(p) \, d\mathbf{x} \, dp \tag{30}$$

297 where the domain $\Omega_{F \cap Z_e}(t)$ is defined in the augmented outcome space of $\mathbf{X}$ and P in terms of the
298 limit-state function:

$$g_{F \cap Z_e}(\mathbf{x}, p, t) = p - p_F(\mathbf{x}, t) \cdot cL(\mathbf{x}, t) \tag{31}$$

299 as $\Omega_{F \cap Z_e}(t) = \{(\mathbf{x}, p) : g_{F \cap Z_e}(\mathbf{x}, p, t) \leq 0\}$.

300 Inserting Equation (29) and Equation (30) into Equation (21) gives:

$$\Pr(F_t | Z_{0:t}) = \frac{\int_{(\mathbf{x}; p) \in \Omega_{F \cap Z_e}(t)} f_{\mathbf{X}}(\mathbf{x}) f_P(p) \, d\mathbf{x} \, dp}{\int_{(\mathbf{x}; p) \in \Omega_{Z_e}(t)} f_{\mathbf{X}}(\mathbf{x}) f_P(p) \, d\mathbf{x} \, dp} = \frac{\Pr\big(g_{F \cap Z_e}(\mathbf{X}, P, t) \leq 0\big)}{\Pr\big(g_{Z_e}(\mathbf{X}, P, t) \leq 0\big)} \tag{32}$$

301 Note that the proportionality constant a vanishes. The numerator and the denominator in Equation
302 (32) correspond to component reliability problems, which can be solved using structural reliability
303 methods.

304 The solution given in Equation (32) can be interpreted as follows. The denominator in Equation
305 (32) corresponds to the probability of an inequality observation event $Z_{e,0:t} = \{g_{Z_e}(\mathbf{X}, P, t) \leq 0\}$
306 and the numerator is equal to the probability of the joint event $F_t \cap Z_{e,0:t} = \{g_{F \cap Z_e}(\mathbf{X}, P, t) \leq 0\}$.
307 In the context of Bayesian updating, the event $Z_{e,0:t}$ is equivalent to the original observation event
308 $Z_{0:t}$ in the sense that:

$$\Pr(F_t | Z_{0:t}) = \Pr(F_t | Z_{e,0:t}) = \frac{\Pr(F_t \cap Z_{e,0:t})}{\Pr(Z_{e,0:t})} \tag{33}$$

309 For applying structural reliability methods, the component reliability problems defined in Equation
310 (32) are also transformed to standard normal space following Section 2.3. The corresponding limit-
311 state functions $G_{F \cap Z_e}$ and G_{Z_e} in $\mathbf{U}$-space are:

$$G_{F \cap Z_e}(\mathbf{u}, t) = u_0 - \Phi^{-1}\big(p_F(\mathbf{T}^{-1}(u_1, \dots, u_n), t) \cdot cL(\mathbf{T}^{-1}(u_1, \dots, u_n), t)\big) \tag{34}$$

312 and

$$G_{Z_e}(\mathbf{u}, t) = u_0 - \Phi^{-1}\big(cL(\mathbf{T}^{-1}(u_1, \dots, u_n), t)\big) \tag{35}$$

313 These limit-state functions respectively describe the domains $\Omega^U_{F \cap Z_e}(t) = \{\mathbf{u} : G_{F \cap Z_e}(\mathbf{u}, t) \leq 0\}$
314 and $\Omega^U_{Z_e}(t) = \{\mathbf{u} : G_{Z_e}(\mathbf{u}, t) \leq 0\}$ in the transformed space. Consequently, the probabilities
315 $\Pr(F_t \cap Z_{e,0:t})$ and $\Pr(Z_{e,0:t})$ can be computed as:

$$\Pr(F_t \cap Z_{e,0:t}) = \Pr(G_{F \cap Z_e}(\mathbf{U}, t) \leq 0) = \int_{\mathbf{u} \in \Omega^U_{F \cap Z_e}(t)} \varphi_{n+1}(\mathbf{u}) \, d\mathbf{u} \tag{36}$$

316 and

$$\Pr(Z_{e,0:t}) = \Pr(G_{Z_e}(\mathbf{U}, t) \leq 0) = \int_{\mathbf{u} \in \Omega^U_{Z_e}(t)} \varphi_{n+1}(\mathbf{u}) \, d\mathbf{u} \tag{37}$$

317 The computation of the integrals in Equations (36) and (37) requires the selection of the constant
318 c. A discussion on how to select c is provided in (Betz et al. 2014b; Au et al. 2015; Straub and
319 Papaioannou 2015b). In the general case, the optimal choice is $c = 1/\sup(L(\mathbf{x}, t))$ where $\sup(\cdot)$
320 is the supremum of the expression $(\cdot)$. In some cases, $\sup(L(\mathbf{x}, t))$ can be readily selected. For
321 instance, in the special case of a single measurement with measurement error E, the supremum of
322 the likelihood function is $\sup(L(\mathbf{x}, t)) = \max(f_E(\epsilon))$ where $f_E(\epsilon)$ is the PDF of E.

4 Computing system failure probabilities with subset simulation

Subset simulation, originally proposed by Au and Beck (2001), is an adaptive Monte Carlo method particularly suitable for evaluating the high-dimensional reliability problems defined in Equations (12), (36) and (37). The method is robust and computationally efficient, and it can be implemented relatively easily. The algorithm is here implemented following Papaioannou et al. (2015).

First, consider the computation of the prior system failure probability $\Pr(F_t) = \Pr(G_F(\mathbf{U}, t) \leq 0)$. The basic idea of subset simulation is to express the event F_t as an intersection of M intermediate events:

$$F_t = E_1 \cap E_2 \cap \ldots \cap E_M \tag{38}$$

The intermediate events are nested, i.e. $E_1 \supset E_2 \supset \cdots \supset E_M = F_t$. Consequently, the probability of the event F_t can be computed by a product of conditional probabilities:

$$\Pr(F_t) = \Pr(E_1 \cap E_2 \cap \ldots \cap E_M) = \prod_{i=1}^{M} \Pr(E_i|E_{i-1}) \tag{39}$$

In this formulation, the event E_0 is the certain event. The intermediate events are selected such that the conditional probabilities $\Pr(E_i|E_{i-1})$, $i = 1, \ldots, M$ are much larger than $\Pr(F_t)$. In this way, the original problem of evaluating the small probability of the rare event F_t reduces to computing a sequence of M larger conditional probabilities.

The intermediate events E_i, $i = 1, \ldots, M$ are defined as $E_i = \{G_F(\mathbf{U}, t) \leq b_i\}$ where $b_1 > b_2 > \cdots > b_M = 0$. The values of b_i are selected adaptively such that the conditional probabilities are equal to a chosen value p_0. For this purpose, N samples of $\mathbf{U}$ are simulated at each subset level i, conditional on the previous intermediate event E_{i-1}. For each generated sample, the limit-state function $G_F(\mathbf{u}, t)$ is evaluated and b_i is set equal to the p_0-percentile of the N resulting values of $G_F(\mathbf{u}, t)$. This procedure is repeated until the p_0-percentile becomes negative. At this stage, the failure event $E_M = F_t$ is reached, for which $b_M = 0$. The samples conditional on the event E_0 are obtained by crude Monte Carlo sampling. The samples conditional on the events E_i, $i = 1, \ldots, M - 1$ are generated by simulating states of Markov chains starting from the samples conditional on E_{i-1}, for which $G_F(\mathbf{u}, t) \leq b_i$. This is achieved by application of Markov Chain Monte Carlo (MCMC) sampling. An estimator $\hat{P}_{SuS}$ of the prior system failure probability $\Pr(F_t)$ can now be written as:

$$\Pr(F_t) \approx \hat{P}_{SuS} = p_0^{M-1}\hat{P}_M \tag{40}$$

$\hat{P}_M$ is the estimate of the conditional probability $\Pr(E_M|E_{M-1})$, which is given by the ratio of the number of samples for which $G_F(\mathbf{u}, t) \leq 0$ over the number of samples N simulated conditional on E_{M-1}.

352 Note that the MCMC samples are generally not statistically independent. Their correlation has an
353 effect on the efficiency and accuracy of subset simulation (see, for example, Au and Beck 2001;
354 Schuëller and Pradlwarter 2007; Papaioannou et al. 2015). It is important to adopt an MCMC
355 sampling algorithm that produces samples with low correlation such that the conditional
356 probabilities $\Pr(E_i|E_{i-1})$ can be estimated with a minimum number of samples. We adopt the
357 adaptive MCMC sampling algorithm of Papaioannou et al. (2015).

358 The value p_0 of the conditional probabilities and the number of simulated samples N at each subset
359 level can be chosen freely. A value of $p_0 = 0.1$ is a suitable choice. N should be selected large
360 enough to give accurate estimates of p_0. Note that the total number of required samples for
361 estimating $\Pr(F_t)$ increases linearly with $-\log_{10}(\Pr(F_t))$ when using subset simulation instead
362 of with $1/\Pr(F_t)$ when using crude Monte Carlo simulation (Au and Beck 2001).

363 The probabilities $\Pr(F_t \cap Z_{e,0:t}) = \Pr(G_{F \cap Z_e}(\mathbf{U}, t) \leq 0)$ and $\Pr(Z_{e,0:t}) = \Pr(G_{Z_e}(\mathbf{U}, t) \leq 0)$ are
364 calculated accordingly. The posterior system failure probability $\Pr(F_t|Z_{0:t})$ is then computed using
365 Equation (21). Alternatively, the conditional probability $\Pr(F_t|Z_{0:t}) = \Pr(F_t|Z_{e,0:t})$ can be
366 estimated directly with a new subset simulation run following the estimation of $\Pr(Z_{e,0:t})$ (see also
367 Schneider et al. 2013; Straub et al. 2016). For this purpose, a set of nested intermediate events
368 $E_0 \supset E_1 \supset \cdots \supset E_M$ is defined where $E_0 = Z_{e,0:t}$, $E_i = \{G_{F \cap Z_e}(\mathbf{U}, t) \leq b_i\}$, $i = 1, \ldots, M$ and $b_1 >$
369 $b_2 > \cdots > b_M = 0$. The conditional probability $\Pr(F_t|Z_{0:t})$ can now be expressed as:

$$\Pr(F_t|Z_{0:t}) = \Pr(E_1 \cap E_2 \cap \ldots \cap E_M|E_0) = \prod_{i=1}^{M} \Pr(E_i|E_{i-1}) \tag{41}$$

370 The first threshold b_1 defining the intermediate event $E_1 = \{G_{F \cap Z_e}(\mathbf{U}, t) \leq b_1\}$ is determined from
371 the samples conditional on $E_0 = Z_{e,0:t}$, which are obtained as a by-product of estimating $\Pr(Z_{e,0:t})$
372 with subset simulation. The remaining thresholds b_i, $i = 2, \ldots, M - 1$ are determined following
373 the original subset simulation procedure. When applying this approach, the estimator $\hat{P}_{SuS}$ defined
374 in Equation (40) provides an estimate of the conditional probability $\Pr(F_t|Z_{0:t})$.

5   Application a: Zayas frame subjected to fatigue deterioration

376 We consider the two-dimensional welded steel frame shown in Figure 1, which is known as Zayas
377 frame (Zayas et al. 1980). The critical load scenario is an environmental load L. In addition, the
378 frame is subjected to fatigue loads throughout its service life of $T = 50$ years. The effect of
379 inspections on the fatigue reliability of the elements and on the reliability of the complete structural
380 system is studied.
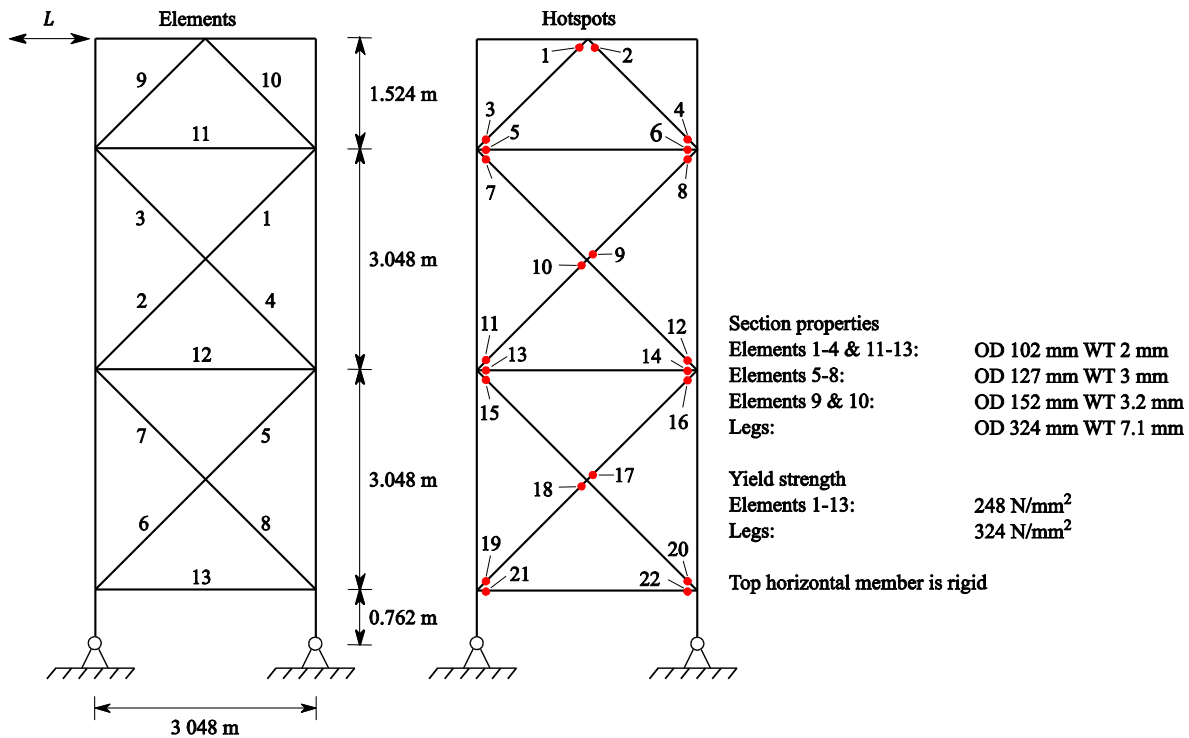
Figure 1. Zayas frame (Zayas et al. 1980). OD is the outer diameter and WT is the wall thickness of the tubular steel members.

5.1 System model

The Zayas frame consists of tubular steel elements with welded connections. The state of fatigue deterioration of any element i depends on the condition of the associated welded connections. Fatigue cracks usually develop at locations with local stress concentrations; welded connections are especially vulnerable due to material inhomogeneities, imperfections, high stress concentrations and residual stresses (Fricke 2003). Locations where fatigue cracks may develop are called hotspots. A welded connection may contain multiple hotspots.

Fatigue crack growth reduces the capacity of welded connections. In the current example, we assume that fatigue deterioration occurs at the welds connecting the braces with the legs and with the upper horizontal element as well as at the welds at the intersection of the X-braces. Furthermore, we assume that each deteriorating welded connection contains only one critical hotspot. Thus, there are $n_E = 13$ deteriorating elements and $n_H = 22$ hotspots as indicated in Figure 1.

The approach of Straub and Der Kiureghian (2011) is adopted to determine the reliability of the welded steel structure subjected to fatigue. At system level, no gradual degradation of weld capacities is considered. At a given time t, a welded connection has either its full capacity or it has completely lost its capacity because of fatigue crack growth. In the current example, we assume that a welded connection loses its capacity if a fatigue crack at any of the associated hotspots grows beyond a critical size (e.g. Madsen 1997). Thus, the deterioration state of any hotspot j at time t

is modeled by a binary random variable $D_{H,j,t}$, where $\{D_{H,j,t} = 1\}$ is the hotspot fatigue damage event and $\{D_{H,j,t} = 0\}$ is the compliment. The event of fatigue damage of hotspot j at time t is defined by a limit-state function $g_{H,j}(\mathbf{x}, t)$ as $\{D_{H,j,t} = 1\} = \{g_{H,j}(\mathbf{X}, t) \leq 0\}$ where $\mathbf{X}$ denotes the vector of all uncertain parameters that describe fatigue deterioration of all hotspots considered in the system reliability analysis. $g_{H,j}(\mathbf{x}, t)$ is written as:

$$g_{H,j}(\mathbf{x}, t) = a_{c,j} - a_j(\mathbf{x}, t) \tag{42}$$

where $a_{c,j}$ is the critical crack size and $a_j(\mathbf{x}, t)$ is the fatigue crack size at hotspot j at time t. $a_j(\mathbf{x}, t)$ is computed by means of a probabilistic fatigue crack growth model presented in Section 5.2. $a_{c,j}$ may be defined such that failure modes such as plastic collapse or unstable crack growth are approximately accounted for.

A structural element loses its capacity if any of the associated welded connections loses its capacity. It follows that an element fails as soon as any of the associated hotspots fails due to fatigue deterioration; this corresponds to a series system. The deterioration state of any element i at time t is, therefore, also modeled by a binary random variable $D_{i,t}$ where $\{D_{i,t} = 1\}$ is the event of element fatigue failure and $\{D_{i,t} = 0\}$ is the compliment. From system reliability theory it follows that the event of fatigue failure of element i can be written as:

$$\{D_{i,t} = 1\} = \bigcup_{j \in C_i}\{D_{H,j,t} = 1\} \tag{43}$$

where C_i is an index set containing the indices of all hotspots associated with element i. The event of fatigue failure of element i can also be expressed by a limit-state function $g_i(\mathbf{x}, t)$ such that $\{D_{i,t} = 1\} = \{g_i(\mathbf{X}, t) \leq 0\}$. $g_i(\mathbf{x}, t)$ is defined as a combination of the individual hotspot limit-state functions $g_{H,j}(\mathbf{x}, t)$, $\forall j \in C_i$ as:

$$g_i(\mathbf{x}, t) = \min_{j \in C_i} g_{H,j}(\mathbf{x}, t) \tag{44}$$

The function h_i defining the relationship between the fatigue model parameters $\mathbf{X}$ and the element deterioration state $D_{i,t}$ can now be written as:

$$D_{i,t} = h_i(\mathbf{X}, t) = I(g_i(\mathbf{X}, t) \leq 0) \tag{45}$$

Using Equation (2), the system deterioration state $\mathbf{D}_t = (D_{1,t}, \dots, D_{n_E,t})$ of the Zayas frame can subsequently be calculated as a function of the uncertain fatigue model parameters $\mathbf{X}$. In the current example, $\mathbf{D}_t$ is a binary random vector with 2^{n_E} states.

The Zayas frame is subjected to a time-variant horizontal load whose annual maximum L has the Gumbel distribution with a coefficient of variation (c.o.v.) $\delta_L = 0.35$. The CDF of L is denoted by

428      $F_L(l)$. Material and geometry properties are modeled as deterministic parameters as listed in Figure
429   1. This simplification is reasonable since the uncertainties associated with these quantities are
430   small compared to the uncertainties associated with the system deterioration state and the load L.
431   It is thus possible to determine a deterministic ultimate horizontal capacity $r(\mathbf{d}_t)$ of the damaged
432   Zayas frame for any realization of the system deterioration state $\mathbf{D}_t = \mathbf{d}_t$. Consequently, the
433   conditional probability of system failure $p_F(\mathbf{x}, t)$ of the Zayas frame corresponds to the probability
434   that the annual maximum load L exceeds the ultimate capacity $r(\mathbf{d}_t)$:

$$\Pr(F_t | \mathbf{D}_t = \mathbf{d}_t) = \Pr(r(\mathbf{d}_t) \leq L) = 1 - F_L(r(\mathbf{d}_t)) \tag{46}$$

435   The mean of L is selected such that the undamaged Zayas frame has an annual probability of
436   system failure $\Pr(F_t | \mathbf{D}_t = \mathbf{0}) = 1.3 \times 10^{-6}$, leading to $\mu_L = 62$ kN.

437   In the current example, $r(\mathbf{d}_t)$ is computed by performing pushover analysis of the structure with
438   all elements damaged according to $\mathbf{D}_t = \mathbf{d}_t$, i.e. all elements with fatigue failure are removed from
439   the model used in the pushover analysis. Through such analyses the ultimate capacity of framed
440   steel structures can be quantified. Non-linear effects associated with non-linear material behavior,
441   imperfections, large displacements and deformations (large strains) are modelled explicitly. The
442   analysis captures load redistribution within the structural system resulting from local stiffness
443   changes. It simulates the collapse process of the structural system including initial yielding,
444   formation of plastic hinges, member buckling as well as formation of a global system collapse
445   mechanism (see e.g. Ultiguide 1999; Skallerud and Amdahl 2002).

446   In the current study, $2^{13} = 8192$ pushover analyses are carried out using USFOS (2014) to pre-
447   calculate the maximum resistance $r(\mathbf{d}_t)$ for all possible realizations of the system deterioration
448   state $\mathbf{D}_t$. The corresponding conditional system failure probabilities $\Pr(F_t | \mathbf{D}_t = \mathbf{d}_t)$ are computed
449   according to Equation (46). These failure probabilities have a reference period $\Delta t = 1$ year but are
450   independent of time. In the subsequent reliability analysis of the deteriorating Zayas frame, the
451   computation of $p_F(\mathbf{x}, t)$ is thus reduced to a lookup operation in which a realization of the fatigue
452   model parameters $\mathbf{x}$ is matched to a pre-calculated conditional system failure probability
453      $\Pr(F_t | \mathbf{D}_t = \mathbf{d}_t)$ at time t by means of Equation (3), i.e. $\mathbf{d}_t = \mathbf{h}(\mathbf{x}, t)$.

454   The influence of individual element failure on the reliability of the Zayas frame depends on the
455   structural importance of the failed element. Following Straub and Der Kiureghian (2011), the
456   structural importance of an element i is quantified in terms of the single-element importance
457   measure SEI_i, which is defined as the difference in the failure probability of the undamaged system
458   and the failure probability of the system in which only element i has failed due to fatigue
459   deterioration.

$$\begin{aligned}
\mathrm{SEI}_i = &\Pr(F_t | D_{1,t} = 0, \ldots, D_{i-1,t} = 0, D_{i,t} = 1, D_{i+1,t} = 0, \ldots, D_{n_E,t} = 0) - \\
&\Pr(F_t | \mathbf{D}_t = \mathbf{0})
\end{aligned} \tag{47}$$

460 Table 1 summarizes the single-element importance measures for all deteriorating elements
461 considered in the system reliability analysis of the Zayas frame.

462 Table 1. Single-element importance (SEI) measure and structural importance category of all deteriorating
463 elements of the Zayas frame.

Element i	SEI_i	Structural importance category
1, 3	1.14×10^{-5}	Medium
2, 4	1.06×10^{-5}	Medium
5, 7	1.99×10^{-3}	High
6, 8	2.00×10^{-3}	High
9, 10	7.25×10^{-7}	Low
11	8.26×10^{-8}	Low
12	6.31×10^{-7}	Low
13	2.27×10^{-7}	Low

464

465 The lower X-braces (elements 5 to 8) are the most important elements followed by the X-braces
466 at the level above (elements 1 to 4). The top braces (elements 9 and 10) and the horizontal braces
467 (elements 11 to 13) are the least important elements.

5.2 Fatigue model

469 In the current example, we adopt the widely used Paris' law (Paris and Erdogan 1963) to describe
470 fatigue crack growth at a given hotspot. For illustration purposes, we consider a through-thickness
471 fatigue crack in an infinite plate subjected to fluctuating stresses in the plane of the plate and
472 orthogonal to the crack. In this case, the fatigue crack is fully characterized by its length $2a$ and
473 Paris' law is written as:

$$\frac{da(n)}{dn} = C \left(\Delta S(n) \sqrt{\pi a(n)} \right)^m \tag{48}$$

474 $da(n)/dn$ is the crack growth rate, n is the number of applied fatigue stress cycles, C and m are
475 empirical material parameters and $\Delta S(n)$ is the varying far-field fatigue stress range. The quantity
476 $\Delta K = \Delta S(n) \sqrt{\pi a(n)}$ is the stress intensity factor (SIF) range. This model can be extended to
477 account for more complex fatigue crack and hotspot geometries as well as more complex fatigue
478 stress distributions (Straub 2004). If desired, the model can be replaced altogether with a more
479 advanced crack growth model (e.g. Altamura and Straub 2014). This will not affect the method as
480 described in the remainder of the paper.

481 Fatigue loads are generally random and the load sequence $\Delta S(n)$ is ideally modeled by a stochastic
482 process (Altamura and Straub 2014). Under the condition that the fatigue stress process is

stationary, ergodic and sufficiently mixing, a simplified approach can be adopted where the crack growth rate $da(n)/dn$ given by Equations (48) is approximated by its expected value with respect to ΔS:

$$\frac{da(n)}{dn} \approx E_{\Delta S}\left[C\left(\Delta S(n)\sqrt{\pi a(n)}\right)^m\right] = C\left(\sqrt{\pi a(n)}\right)^m E_{\Delta S}[\Delta S(n)^m] \tag{49}$$

The fatigue stress process is described by its stationary distribution $f_{\Delta S}(\Delta S)$ and an annual stress cycle rate ν (e.g. Madsen et al. 1986). The quantity $\Delta S_e = (E_{\Delta S}[\Delta S(n)^m])^{1/m}$ is interpreted as an equivalent stress range. In the current example, we assume that the stationary distribution of the fatigue stress ranges $f_{\Delta S}(\Delta S)$ can be modeled by a Weibull distribution. The equivalent stress range is hence given by:

$$\Delta S_e = (E_{\Delta S}[\Delta S(n)^m])^{1/m} = k\Gamma\left(1 + \frac{m}{\lambda}\right)^{1/m} \tag{50}$$

$\Gamma(\cdot)$ denotes the Gamma function and k and λ are the Weibull scale and shape parameters. k is modeled as a lognormal random variable to model statistical uncertainties in the calculation of ΔS_e; λ is assumed to be deterministic.

The parameters C and m of Paris' law are modeled as time-invariant random variables to capture uncertainties due to the variability of the material properties and material inhomogeneities. Proper attention has to be paid to modeling the correlation among C and m. They are empirical parameters generally derived from the same experiments and are therefore strongly correlated. To model the dependence among the Paris' law parameters, the linear relationship between $\ln C$ and m given in (Gurney 1978) is adopted:

$$\ln C = -15.84 - 3.34m \tag{51}$$

Equation (51) is valid if stresses are given in N/mm^2 and the crack growth rate is given in m/cycle. In the following, C is modeled as a lognormally distributed random variable. m is thus normal distributed due to the linear relationship between $\ln C$ and m.

To capture uncertainties in the fabrication quality, the initial crack size a_0 is modeled as a random variable with exponential distribution. Uncertainties in the calculation of the hotspot stress and in the calculation of the SIF range are captured by introducing lognormal random bias factors $B_{\Delta S}$ and B_{SIF}, which are multiplied with the calculated equivalent stress range ΔS_e. The one-dimensional crack growth model given in Equation (48) is rewritten as:

$$\frac{da(n)}{dn} = C\left(B_{SIF}B_{\Delta S}\Delta S_e\sqrt{\pi a(n)}\right)^m \tag{52}$$

508 With $a_j(n = 0) = a_{0,j}$ as initial condition, the differential equation given by Equation (52) is
509 solved for the fatigue crack size a_j at hotspot j as a function of time t (Madsen et al. 1986):

$$a_j(\mathbf{X}, t) = \begin{cases} \left[\left(1 - \frac{m_j}{2}\right) C_j B_{SIF,j}^{m_j} B_{\Delta S,j}^{m_j} \Delta S_{e,j}^{m_j} \pi^{\frac{m_j}{2}} v_j t + a_{0,j}^{\left(1 - \frac{m_j}{2}\right)} \right]^{\left(1 - \frac{m_j}{2}\right)^{-1}}, & m_j \neq 2 \\ a_{0,j} \exp\left(C_j B_{SIF,j}^2 B_{\Delta S,j}^2 \Delta S_{e,j}^2 \pi v_j t\right), & m_j = 2 \end{cases} \quad (53)$$

510 where t is the time in years, v_j is the annual stress cycle rate and $v_j t$ is the total number of stress
511 cycles in the period $[0, t]$. $\Delta S_{e,j}$ is computed as a function of k_j, λ_j and m_j according to Equation
512 (50). The vector of all uncertain parameters describing fatigue deterioration of all hotspots
513 considered in the system reliability analysis is defined as:

$$\mathbf{X} = \left(C_1, m_1, a_{0,1}, B_{SIF,1}, B_{\Delta S,1}, k_1, \dots, C_{n_H}, m_{n_H}, a_{0,n_H}, B_{SIF,n_H}, B_{\Delta S,n_H}, k_{n_H}\right) \quad (54)$$

514 The same probabilistic models are applied to describe the crack growth model parameters for all
515 hotspots $j = 1, \dots, n_H$. They are summarized in Table 2.

516 Table 2. Probabilistic models of the fatigue crack growth parameters for all hotspots $j = 1, \dots, n_H$.

Parameter	Dimension	Distribution	Mean	Standard deviation
$\ln k_j$	corresponding to N/mm^2	normal	2.0	0.275
λ_j	-	deterministic	0.8	-
v_j	yr^{-1}	deterministic	$5 \cdot 10^6$	-
$a_{0,j}$	mm	exponential	0.11	0.11
$a_{c,j}$	mm	deterministic	20	-
$\ln C_j$	corresponding to N and mm	normal	-29.97	0.514
m_j	-	normal	calculated from $\ln C_j = -15.84 - 3.34 m_j$	
$B_{\Delta S,j}$	-	lognormal	1.0	0.1
$B_{SIF,j}$	-	lognormal	1.0	0.1

517

518 The mean and standard deviation of the equivalent stress range $\Delta S_{e,j}$ are a function of the
519 distributions of $\ln k_j$ and $\ln C_j$ through Equations (50) and (51). They are $\mu_{\Delta S_{e,j}} = 20.1$ N/mm^2
520 and $\sigma_{\Delta S_{e,j}} = 5.65$ N/mm^2.

521 Statistical dependence among hotspot fatigue behavior is modeled through correlation coefficients
522 among the fatigue model parameters. In the current example, the fatigue model parameters $a_{0,j}$,
523 C_j, k_j, $B_{\Delta S,j}$ and $B_{SIF,j}$ are equi-correlated among all hotspots $j = 1, \dots, n_H$ with correlation
524 coefficients ρ_{a_0}, $\rho_{\ln C}$, $\rho_{\ln k}$, $\rho_{B_{\Delta S}}$ and $\rho_{B_{SIF}}$. The correlation coefficient ρ_{a_0} represents the
525 statistical dependence due to common fabrication quality; $\rho_{\ln C}$ reflects the statistical dependence

526 due to common material characteristics; $\rho_{\ln k}$ models the statistical dependence due to common
527 loading characteristics; and $\rho_{B_{\Delta S}}$ and $\rho_{B_{SIF}}$ describe statistical dependence due to common
528 uncertainties in the calculation of hotspot fatigue stress ranges and SIF ranges. The joint
529 distribution of all fatigue model parameters in **X** is subsequently modeled through a Gaussian
530 copula (Nataf) model (Liu and Der Kiureghian 1986).

531 To study the influence of different levels of statistical dependence among hotspot fatigue behavior,
532 three different dependence cases are considered (low, medium, high), which are defined in terms
533 of the correlation coefficients ρ_{a_0}, $\rho_{\ln C}$, $\rho_{\ln k}$, $\rho_{B_{\Delta S}}$ and $\rho_{B_{SIF}}$ as listed in Table 3.

534 Table 3. Correlation coefficients among the fatigue crack growth parameters.

	low dependence	medium dependence	high dependence
ρ_{a_0}	0.2	0.5	0.8
$\rho_{\ln C}$	0.2	0.5	0.8
ρ_{lnk}	0.2	0.5	0.8
$\rho_{B_{\Delta S}}$	0.2	0.5	0.8
$\rho_{B_{SIF}}$	0.2	0.5	0.8

5.3 Inspection model

536 In the context of fatigue deterioration, relevant inspection outcomes are (a) no detection, (b)
537 detection but no measurement, and (c) detection and measurement of a fatigue crack. These
538 inspection outcomes are directly related to the crack size $a_j(\mathbf{X}, t)$ predicted for a given hotspot j
539 at inspection time t. In the current study, we consider inspection outcomes of the type (a) and (b).
540 The ability of an inspection method to detect a fatigue crack with a certain size $A = a$ is commonly
541 described by a probability of detection curve $\pi(a)$, which is defined as:

$$\pi(a) = \Pr(\text{detection of a fatigue crack}|A = a) \tag{55}$$

542 Such a probability of detection curve describes the performance of the applied inspection method;
543 it accounts for uncertain factors such as measurement errors, inspector performance and
544 environmental conditions (Straub 2004). In the current case study, an exponential probability of
545 detection curve is applied:

$$\pi(a) = 1 - \exp(-a/\lambda_D) \tag{56}$$

546 with $\lambda_D = 1.95$ mm. This probability of detection model is representative of magnetic particle
547 inspection (Moan et al. 2000).

548 The likelihood function describing the inspection outcome $Z_i(t) = \{$fatigue crack detected at
549 hotpot j at time $t\}$ is thus equal to the probability of detection:

$$L_i(\mathbf{x}, t) = \pi\left(a_j(\mathbf{x}, t)\right) \tag{57}$$

The likelihood function of the complementary inspection outcome $Z_i(t) = \{$no fatigue crack detected at hotpot j at time $t\}$ is:

$$L_i(\mathbf{x}, t) = 1 - \pi\left(a_j(\mathbf{x}, t)\right) \tag{58}$$

Under the common assumption that individual inspection outcomes are statistically independent given the crack sizes $a_j(\mathbf{x}, t), j = 1, \ldots, n_H$, the combined likelihood function $L(\mathbf{x}, t)$ of all inspection outcomes $Z_{0:t}$ in the time period $[0, t]$ is given by Equation (20). If individual inspections are not statistically independent due to, for example, common influencing factors such as environmental conditions and inspector characteristics, the combined likelihood has to be formulated such that this aspect is captured. Approaches to modeling dependence among inspection outcomes are, for example, presented in (Straub and Faber 2003)(Maljaars and Vrouwenvelder 2014).

Since detection/no-detection events provide inequality information, the constant c that ensures $0 \le cL(\mathbf{x}, t) \le 1$ for all $\mathbf{x}$ can be chosen as $c = 1$ (see also Section 3.1).

5.4 Prior system reliability analysis

The prior annual system failure probability $\Pr(F_t)$ of the Zayas frame is computed for each degree of dependence among hotspot fatigue behavior according to Equation (12). The results are shown in Figure 2. The problem is solved using subset simulation as described in Section 4 with conditional probabilities $p_0 = 0.1$ and $N = 1000$ samples per subset level. The statistics of the system failure probability are determined from 500 independent simulation runs. This approach is applied in all subsequent analyses presented in this paper.
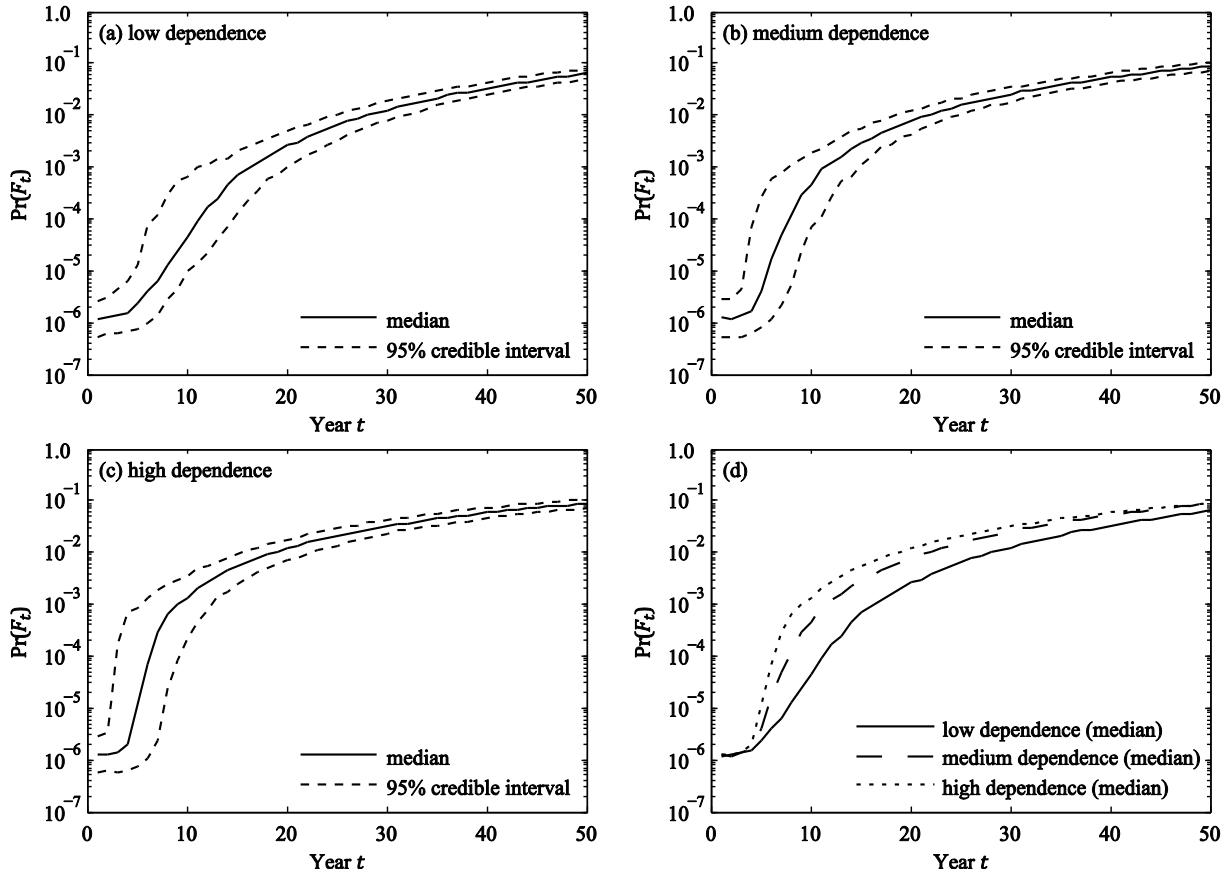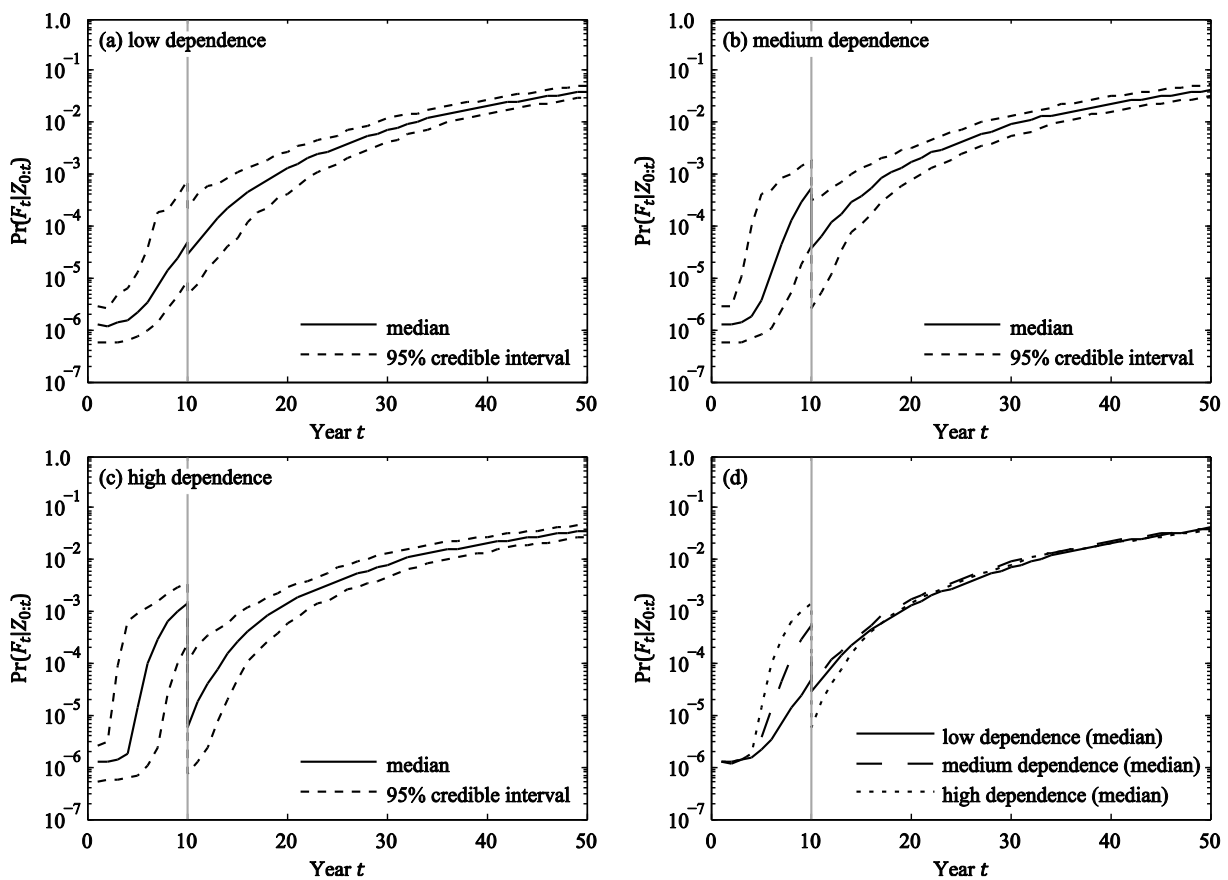
Figure 2. Median and 95% credible interval of the prior annual system failure probability $\Pr(F_t)$ of the Zayas frame as a function of different degrees of dependence among hotspot fatigue behavior. Computations are performed with subset simulation as summarized in Section 4 with conditional probabilities $p_0 = 0.1$ and $N = 1000$ samples per subset level. (d) compares the respective medians of the prior annual system failure probability.

As expected, the annual system failure probability $\Pr(F_t)$ increases with time t, due to fatigue deterioration. Furthermore, Figure 2(d) indicates that a higher dependence among hotspot fatigue behavior leads to a larger system failure probability due to an increase in the probability of joint occurrence of several element fatigue failures. This result is expected for a redundant structural system (Straub and Der Kiureghian 2011).

The width of the 95% credible interval indicates the accuracy of the employed subset simulation. The interval has 0.95 probability of containing the true value of the system failure probability (within the confines of the model). From Figure 2(a) to (c) it can be seen that the accuracy of the computation varies with time t since the number of samples per subset level used in the simulation is the same for all years. Results are less accurate for low values of t, because of the associated smaller system failure probability. Note, however, that the variability of the simulated failure probabilities at the beginning of the structure's service life ($t < 5$yr) is small. In this period, the probability of fatigue failures is very small, and they have little effect on the system failure probability (the failure probability of the undamaged Zayas frame is $\Pr(F_t|\mathbf{D}_t = \mathbf{0}) = 1.3 \cdot 10^{-6}$).

5.5   Posterior system reliability analysis

In this section, different inspection scenarios in terms of inspection times, coverage and outcomes are considered to study their effect on the reliability of the Zayas frame. Firstly, hotspots $\{5, 6, 13, 14, 21, 22\}$ are inspected at time $t = 10$ years. These hotspots are associated with the least important braces of the Zayas frame (see Figure 1 and Table 1). No fatigue cracks are detected during the inspection. The posterior annual system failure probability $\Pr(F_t|Z_{0:t})$, $t = 1, \ldots, 50$ are computed for each degree of dependence among hotspot fatigue behavior with subset simulation as described in Section 4 with conditional probabilities $p_0 = 0.1$ and $N = 1000$ samples per subset level. The results are shown in Figure 3.

Figure 3. Median and 95% credible interval of the posterior annual system failure probability $\Pr(F_t|Z_{0:t})$ of the Zayas frame as a function of different degrees of dependence among hotspot fatigue behavior. Hotspots $\{5, 6, 13, 14, 21, 22\}$ are inspected at time $t = 10$ years. No fatigue cracks are detected. Computations are performed with subset simulation as summarized in Section 4 with conditional probabilities $p_0 = 0.1$ and $N = 1000$ samples per subset level. (d) compares the respective medians of the posterior annual system failure probability.

When considering the posterior medians of the estimated posterior system failure probabilities shown in Figure 3 (a) to (c), it can be seen that the system failure probability reduces after the inspection due to the positive inspection result. The effect increases with increasing degree of dependence among hotspot deterioration behavior.

607 Table 4 lists the probabilities $\Pr(Z_{e,0:t})$ and $\Pr(F_t|Z_{0:t})$ computed at time $t = 10$ years. The subset
608 simulation (SuS) results are presented together with those from additional Monte Carlo simulations
609 (MCS). The number of model evaluations is also provided for each simulation of $\Pr(F_t|Z_{0:t})$ to
610 indicate the computational efforts, since the accuracy can always be improved by increasing the
611 number of samples. The results in Table 4 show that the probability of the inspection outcome is
612 large. This is because the initial defects at each hotspot considered in the current case study are
613 small, and hence the fatigue cracks are unlikely to grow to a detectable size within the first 10
614 years of the structure's service life.

615 Table 4 Probability of the inspection outcome $\Pr(Z_{e,0:t})$ and the posterior system failure probability
616 $\Pr(F_t|Z_{0:t})$ at time $t = 10$ years. Subset simulation (SuS) is performed as summarized in Section 4 with
617 conditional probabilities $p_0 = 0.1$ and $N = 1000$ samples per subset level. Results in square brackets
618 represent the 95% credible interval. MCS is performed with 10^7 samples. Results are shown as 95%
619 confidence interval. The total number of model runs are provided for the computation of $\Pr(Z_{e,0:t})$ and
620 $\Pr(F_t|Z_{0:t})$.

Case	Method	$\Pr(Z_{e,0:t})$	$\Pr(F_t|Z_{0:t})$	# model runs
Low dependence	SuS	$[0.642; 0.7]$	$[0.0467; 2.3] \cdot 10^{-4}$	$5.9 \cdot 10^3$
	MCS	$[0.671; 0.6716]$	$[7.08; 8.49] \cdot 10^{-5}$	10^7
Medium dependence	SuS	$[0.659; 0.717]$	$[0.0267; 3.11] \cdot 10^{-4}$	$5.9 \cdot 10^3$
	MCS	$[0.6875; 0.688]$	$[0.864; 1.01] \cdot 10^{-4}$	10^7
High dependence	SuS	$[0.673; 0.734]$	$[0.00758; 1.08] \cdot 10^{-4}$	$6.8 \cdot 10^3$
	MCS	$[0.7042; 0.7048]$	$[2.94; 3.79] \cdot 10^{-5}$	10^7

621

622 In the second example, hotspots {15,16,17,18,19,20} are inspected at time $t = 10$ years. These
623 hotspots are associated with the most important structural members of the Zayas frame (see Figure
624 1 and Table 1). We assume again that each inspection results in a no-detection event. The posterior
625 annual system failure probability $\Pr(F_t|Z_{0:t})$ is shown for all three dependence cases in Figure 4.
626 In contrast to the first scenario, an inspection of the most important structural elements has a
627 significant effect on the system reliability regardless of the degree of dependence among element
628 deterioration.

629
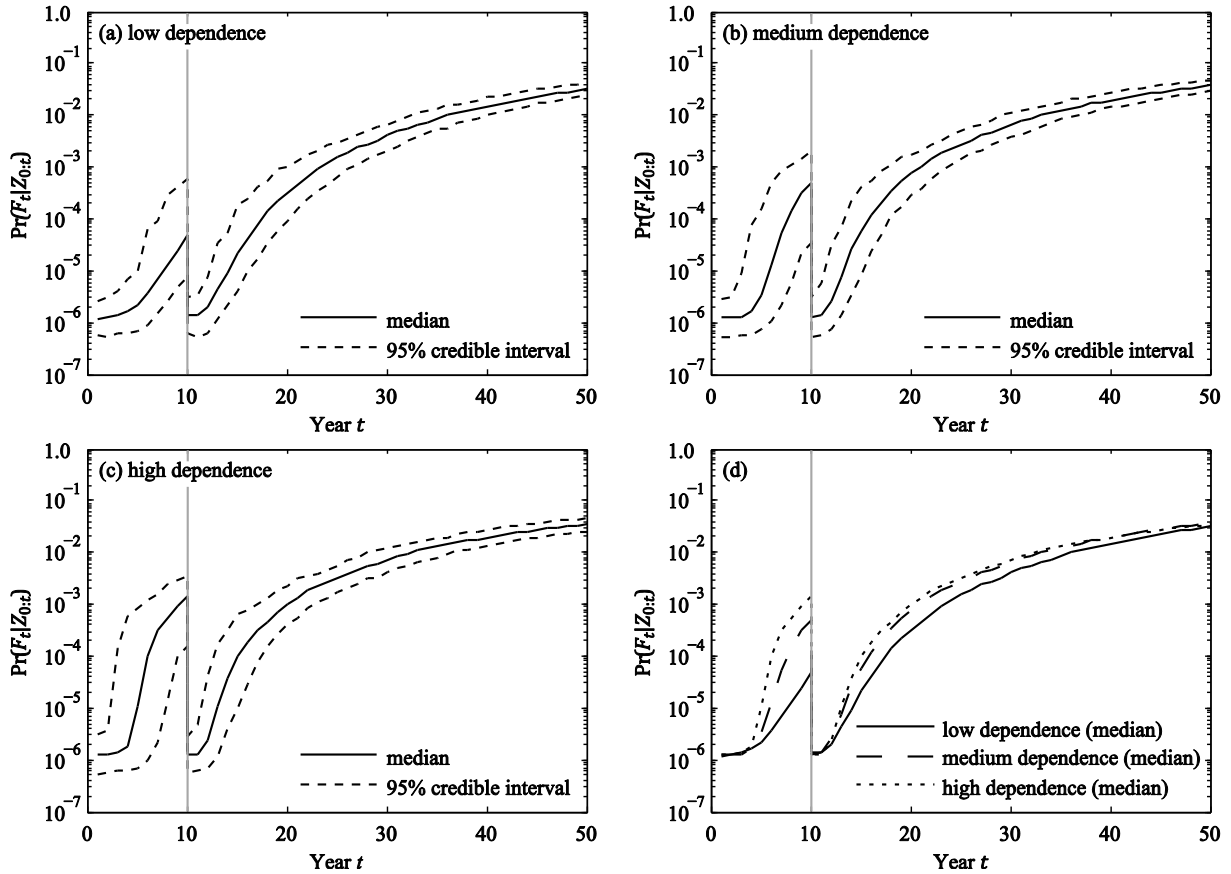
Figure 4. Median and 95% credible interval of the posterior annual system failure probability $\Pr(F_t|Z_{0:t})$ of the Zayas frame as a function of different degrees of dependence among hotspot fatigue behavior. Hotspots $\{15,16,17,18,19,20\}$ are inspected at time $t = 10$ years. No fatigue cracks are detected. Computations are performed with subset simulation as summarized in Section 4 with conditional probabilities $p_0 = 0.1$ and $N = 1000$ samples per subset level. (d) compares the respective medians of the posterior annual system failure probability.

The probability of the inspection outcome $\Pr(Z_{e,0:t})$ and the posterior system failure probability $\Pr(F_t|Z_{0:t})$ at year 10 are summarized in Table 5 for each dependence case. The computed probabilities $\Pr(Z_{e,0:t})$ are the same as in the first scenario (see Table 4) because the applied probabilistic models of the crack growth parameters are identical for all hotspots (see Table 2). Comparing the bounds of the SuS and MCS results for $\Pr(F_t|Z_{0:t})$, it is seen that their accuracy is similar even though the number of samples in the SuS is only $N = 1000$ samples per subset level.

642　Table 5. Probability of the inspection outcome $\Pr(Z_{e,0:t})$ and the posterior system failure probability
643　$\Pr(F_t|Z_{0:t})$ at time $t = 10$ years. Subset simulation is performed as summarized in Section 4 with
644　conditional probabilities $p_0 = 0.1$ and $N = 1000$ samples per subset level. Results represent the 95%
645　credible interval. MCS is performed with 10^7 samples. Results represent the 95% confidence interval.

Case	Method	$\Pr(Z_{e,0:t})$	$\Pr(F_t|Z_{0:t})$	# model runs
Low dependence	SuS	$[0.642; 0.701]$	$[0.635; 3.15] \cdot 10^{-6}$	$6.8 \cdot 10^3$
	MCS	$[0.671; 0.6716]$	$[1.22; 3.54] \cdot 10^{-6}$	10^7
Medium dependence	SuS	$[0.656; 0.715]$	$[0.543; 3.12] \cdot 10^{-6}$	$6.8 \cdot 10^3$
	MCS	$[0.6876; 0.6882]$	$[1.89; 4.53] \cdot 10^{-6}$	10^7
High dependence	SuS	$[0.673; 0.73]$	$[0.55; 2.77] \cdot 10^{-6}$	$6.8 \cdot 10^3$
	MCS	$[0.7042; 0.7048]$	$[1.06; 3.2] \cdot 10^{-6}$	10^7

646

647　In the third scenario, hotspots {15,16,17,18,19,20} are again inspected in year 10. No fatigue
648　cracks are detected at hotspots {15,16,17,18} whereas defects are detected at hotspots {19,20}.
649　The corresponding posterior annual system failure probabilities are shown for all three dependence
650　cases in Figure 5. The system failure probability increases after the inspection since fatigue cracks
651　are detected in welds connecting two of the most important braces with the legs (see Figure 1 and
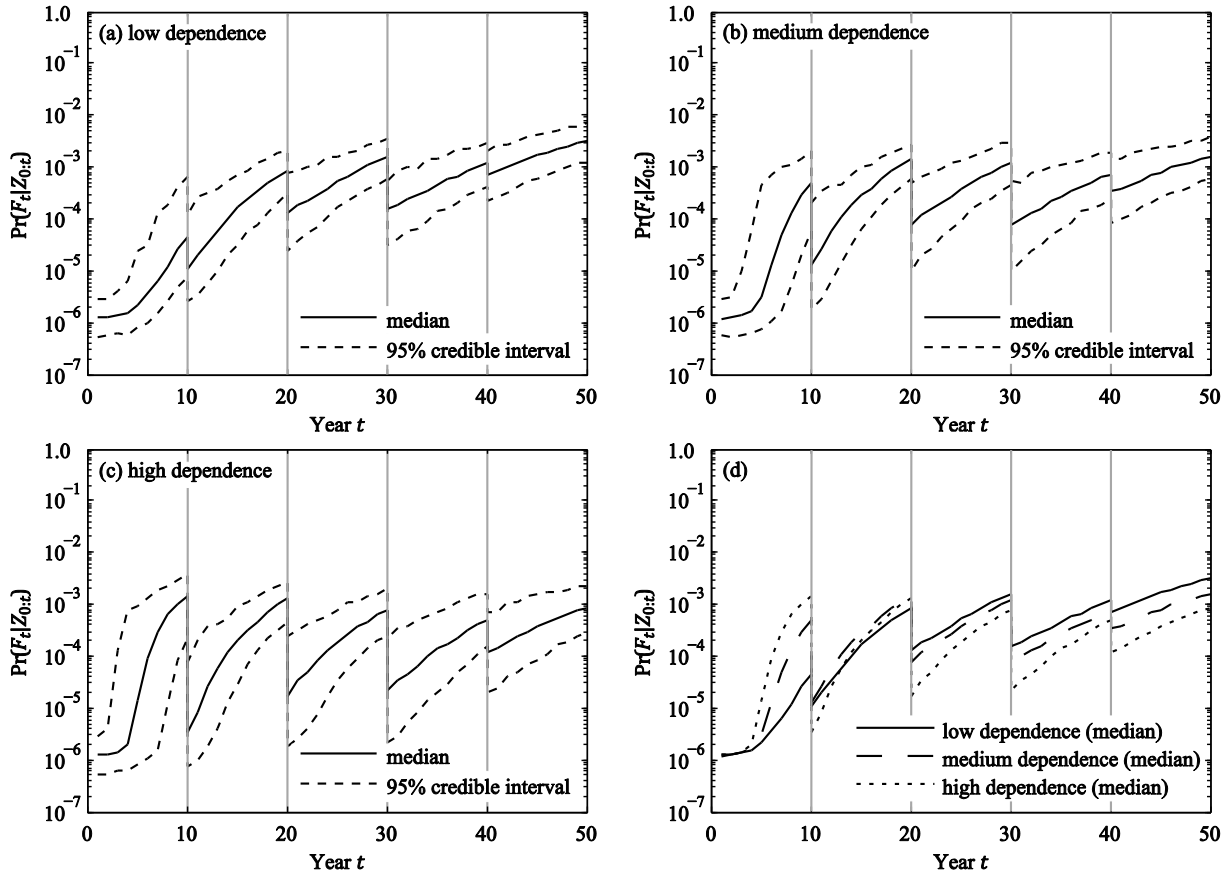652　Table 1). The effect is most pronounced in the low dependence case.

653
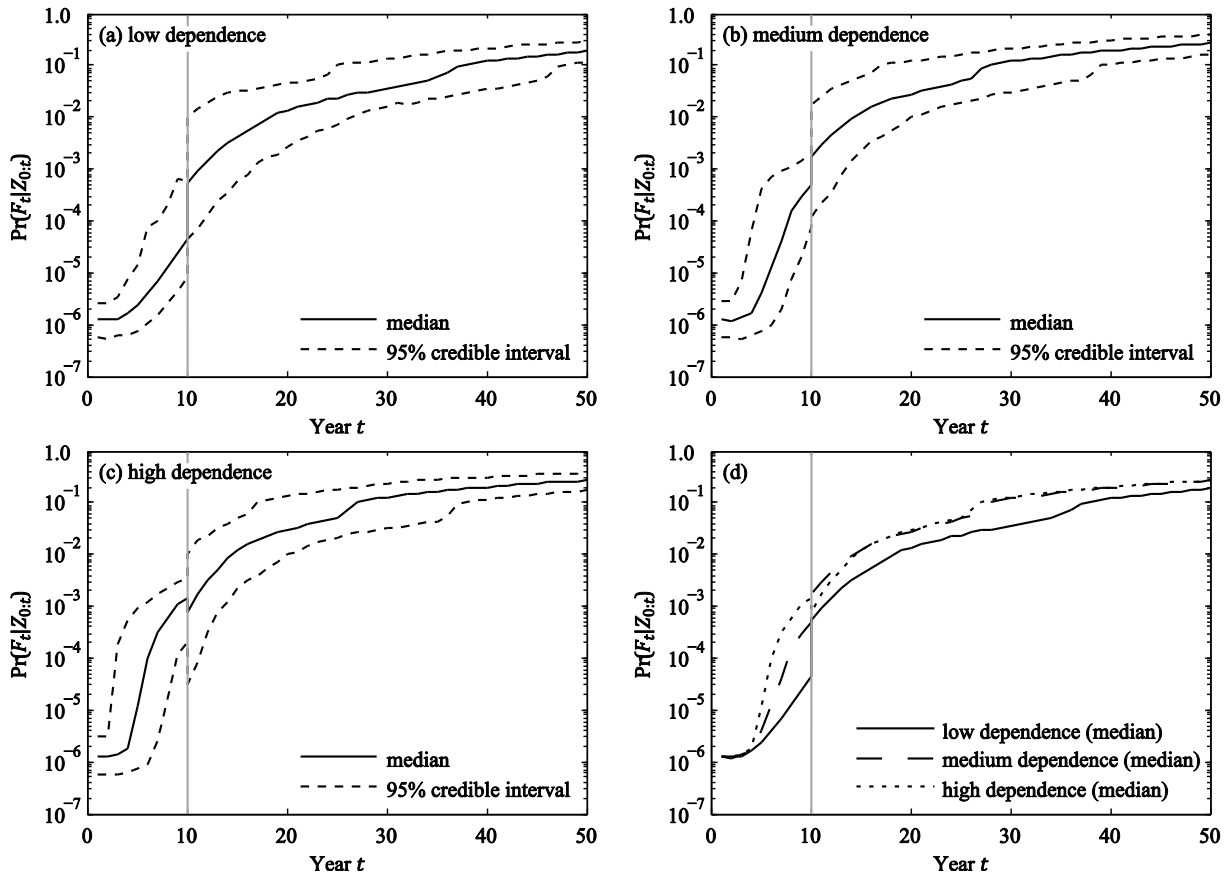
Figure 5. Median and 95% credible interval of the posterior annual system failure probability $\Pr(F_t|Z_{0:t})$ of the Zayas frame as a function of different degrees of dependence among hotspot fatigue behavior. Hotspots {15,16,17,18,19,20} are inspected in year 10. No fatigue cracks are detected at hotspots {15,16,17,18} whereas defects are detected at hotspots {19,20}. Computations are performed with subset simulation as summarized in Section 4 with conditional probabilities $p_0 = 0.1$ and $N = 1000$ samples per subset level. (d) compares the respective medians of the posterior annual system failure probability.

Table 6 shows that the current inspection outcome is approximately two orders of magnitude less probable than the no-detection outcomes in the previous scenarios (see Table 4 and Table 5). When comparing the subset simulation results in Table 5 and Table 6, it can also be seen that the number of model evaluations are similar in both examples although the posterior system failure probabilities $\Pr(F_t|Z_{0:t})$ are multiple orders of magnitude larger in the current example. The reason is that the simulations of the smaller probabilities of the observation event $\Pr(Z_{e,0:t})$ require here more model evaluations.

667 Table 6. Probability of the inspection outcome $\Pr(Z_{e,0:t})$ and the posterior system failure probability
668 $\Pr(F_t|Z_{0:t})$ at time $t = 10$ years. Subset simulation is performed as summarized in Section 4 with
669 conditional probabilities $p_0 = 0.1$ and $N = 1000$ samples per subset level. Results represent the 95%
670 credible interval. MCS is performed with 10^7 samples. Results represent the 95% confidence interval.

Case	Method	$\Pr(Z_{e,0:t})$	$\Pr(F_t|Z_{0:t})$	# model runs
Low dependence	SuS	$[2.45; 5.18] \cdot 10^{-3}$	$[0.00429; 1.02] \cdot 10^{-2}$	$7.1 \cdot 10^3$
	MCS	$[3.66; 3.74] \cdot 10^{-3}$	$[2.64; 3.79] \cdot 10^{-3}$	10^7
Medium dependence	SuS	$[2.66; 5.71] \cdot 10^{-3}$	$[0.0121; 1.67] \cdot 10^{-2}$	$6.2 \cdot 10^3$
	MCS	$[3.82; 3.9] \cdot 10^{-3}$	$[6.14; 7.79] \cdot 10^{-3}$	10^7
High dependence	SuS	$[2.57; 5.78] \cdot 10^{-3}$	$[0.0319; 9.84] \cdot 10^{-3}$	$7.0 \cdot 10^3$
	MCS	$[3.86; 3.93] \cdot 10^{-3}$	$[2.96; 4.13] \cdot 10^{-3}$	10^7

671

672 In the last scenario, regular inspections are performed at 10 year intervals. Hotspots associated
673 with elements of each importance category are inspected at each inspection apart from the last
674 inspection where only hotspots associated with the upper braces (low importance category) are
675 inspected (see Figure 1 and Table 1). This inspection strategy ensures that each hotspot is inspected
676 at least once throughout the service life of the structure. The inspection strategy is as follows:
677 hotspots {15,16,7,8,5,6} are inspected at time $t = 10$ years, hotspots {17,18,9,10,13,14} are
678 inspected at time $t = 20$ years, hotspots {19,20,11,12,21,22} are inspected at time $t = 30$ years
679 and hotspots {1,2,3,4} are inspected at time $t = 40$ years. Each inspection results in a no-detection
680 events. The results are shown in Figure 6. As expected, the positive inspection outcome causes a
681 reduction in the annual system failure probability after each inspection. This effect increases with
682 increasing degree of dependence among hotspot fatigue behavior.

Figure 6. Median and 95% credible interval of the posterior annual system failure probability $\Pr(F_t|Z_{0:t})$ of the Zayas frame as a function of different degrees of dependence among hotspot fatigue behavior. Hotspots {15,16,7,8,5,6} are inspected at time $t = 10$ years, hotspots {17,18,9,10,13,14} are inspected at time $t = 20$ years, hotspots {19,20,11,12,21,22} are inspected at time $t = 30$ years and hotspots {1,2,3,4} are inspected at time $t = 40$ years. No fatigue cracks are detected. Computations are performed with subset simulation as summarized in Section 4 with conditional probabilities $p_0 = 0.1$ and $N = 1000$ samples per subset level. (d) compares the respective medians of the posterior annual system failure probability.

Table 7 summarizes the median probability of the inspection outcome $\Pr(Z_{e,0:t})$ after each inspection. Each additional inspection provides more information on the actual condition of the structure. With increasing amount of information, the probability of the inspection outcome $\Pr(Z_{e,0:t})$ decreases. It also decreases with decreasing degree of dependence among hotspot fatigue behavior.

Table 7. Median of the probability of the inspection outcome $\Pr(Z_{e,0:t})$ as a function of the number of
inspections and the degree of dependence among hotspot fatigue behavior.

Year t	low dependence	medium dependence	high dependence
10	0.67	0.69	0.70
20	0.42	0.47	0.52
30	0.25	0.33	0.40
40	0.17	0.26	0.34

6 Application b: Daniels system subjected to fatigue deterioration

We apply the proposed approach to the idealized structural system shown in Figure 7, known as
Daniels system (Daniels 1945). We here assume that the Daniels system consists of welded steel
members, which are subjected to fatigue deterioration throughout the structure's service life of
$T = 50$ years. The properties of the Daniels system, in particular the exchangeability of the
elements, facilitate numerical investigations.
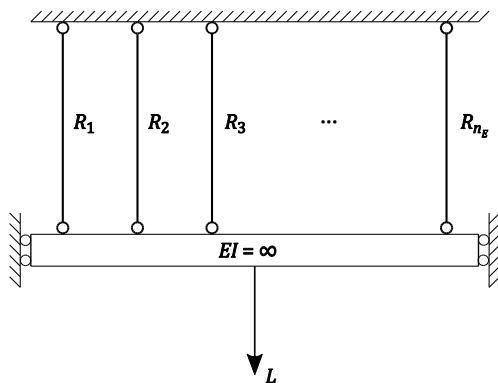
Figure 7. Daniels system with n_E elements.

6.1 System model

The considered Daniels system consists of $n_E = 100$ elements with independent and identically
distributed (i.i.d.) capacities R_i, $i = 1, \ldots, n_E$. The applied load is shared equally among all
elements; its annual maximum is denoted by L. In the current example, we assume that each
element is associated with one welded connection. Furthermore, we assume that each welded
connection contains only one critical hotspot, i.e. $n_H = n_E = 100$.

The same deterioration model presented in Section 5 is applied to model fatigue deterioration of
the Daniels system. At any time t there are $N_{F,t}$ failed elements and $n_E - N_{F,t}$ elements are
available to resist the applied loads. Because of the exchangeability of its elements, $N_{F,t}$ represents
the deterioration state of the Daniels system at time t. $N_{F,t}$ is computed as a function h of the
deterioration model parameters $\mathbf{X}$ as:

$$N_{F,t} = h(\mathbf{X}, t) = \sum_{i=1}^{n_E} I(g_i(\mathbf{X}, t) \leq 0) \tag{59}$$

716   where $g_i(\mathbf{X}, t)$ is the limit-state function defining the event of fatigue failure of element i; see
717   Equation (44). The system failure probability of the Daniels system in the reference period $[t - $
718    $\Delta t, t]$ conditional on a realization of the fatigue model parameters $\mathbf{X} = \mathbf{x}$ can now be written as:

$$p_F(\mathbf{x}, t) = \Pr\left(F_t | N_{F,t} = h(\mathbf{x}, t)\right) \tag{60}$$

719   For given probability distributions of the component capacities R_i and the annual maximum load
720   L, the conditional system failure probability $\Pr(F_t | N_{F,t} = k)$, $k = 0, \ldots, n_E$ is readily determined
721   from Daniels system formulation. This failure probability has a reference period $\Delta t = 1$ year but
722   it is independent of time t. For ductile element behavior (steel elements), the solution is given by
723   (Gollwitzer and Rackwitz 1990):

$$\Pr(F_t | N_{F,t} = k) = \Pr\left(\sum_{i=1}^{n_E - k} R_i \leq L\right) \tag{61}$$

724   The right hand side of Equation (61) corresponds to a component reliability problem, which can
725   be solved using structural reliability methods.

726   In the current example, the component capacities R_i, $i = 1, \ldots, n_E$ are modeled as i.i.d. normal
727   random variables with c.o.v. $\delta_R = 0.15$. The annual maximum of the applied load L is modeled as
728   a lognormal random variable with c.o.v. $\delta_L = 0.25$. The ratio of the mean values of $n_E R_i$ and L is
729   selected such that the undamaged Daniels system has a probability of failure $\Pr(F_t | N_{F,t} = 0) = $
730   1.3×10^{-6}. The resulting ratio is $n_E \mu_{R_i} / \mu_L = 3.09$. $\Pr(F_t | N_{F,t} = k)$, $k = 0, \ldots, n_E$ is pre-
731   calculated for each realization of the system deterioration state by solving Equation (61) using the
732   first-order reliability method (FORM). The results are illustrated in Figure 8. In the subsequent
733   reliability analysis of the deteriorating Daniels system, the computation of $p_F(\mathbf{x}, t)$ is again
734   reduced to a lookup operation.
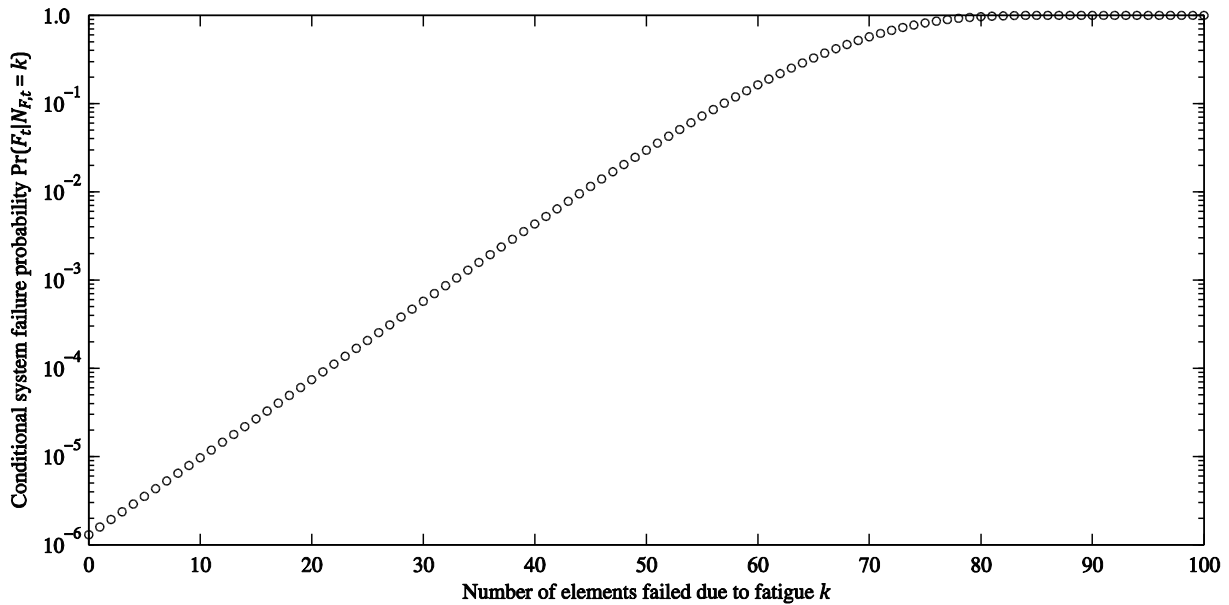
Figure 8. Failure probability of the Daniels system as a function of the number of elements failed due to
736 fatigue.

737 Each element of the Daniels system is equally important due to the perfect load sharing among the
738 structural elements. The single element importance measure of an individual element i of the
739 Daniels system is $\text{SEI}_i = \Pr\left(F_t|N_{F,t} = 1\right) - \Pr\left(F_t|N_{F,t} = 0\right) = 2.9 \times 10^{-7}$. The Daniels system
740 is highly redundant with respect to single element failure when compared to the Zayas frame
741 studied in Section 5 where failure of elements of the highest importance category lead to a
742 significant reduction in system reliability, see Table 1.

6.2   Prior system reliability analysis

744 The computed prior annual system failure probability $\Pr(F_t)$ of the Daniels system is shown in
745 Figure 9 for each degree of dependence among hotspot fatigue. Computations are performed with
746 subset simulation as summarized in Section 4 with conditional probabilities $p_0 = 0.1$ and $N =$
747 1000 samples per subset level.
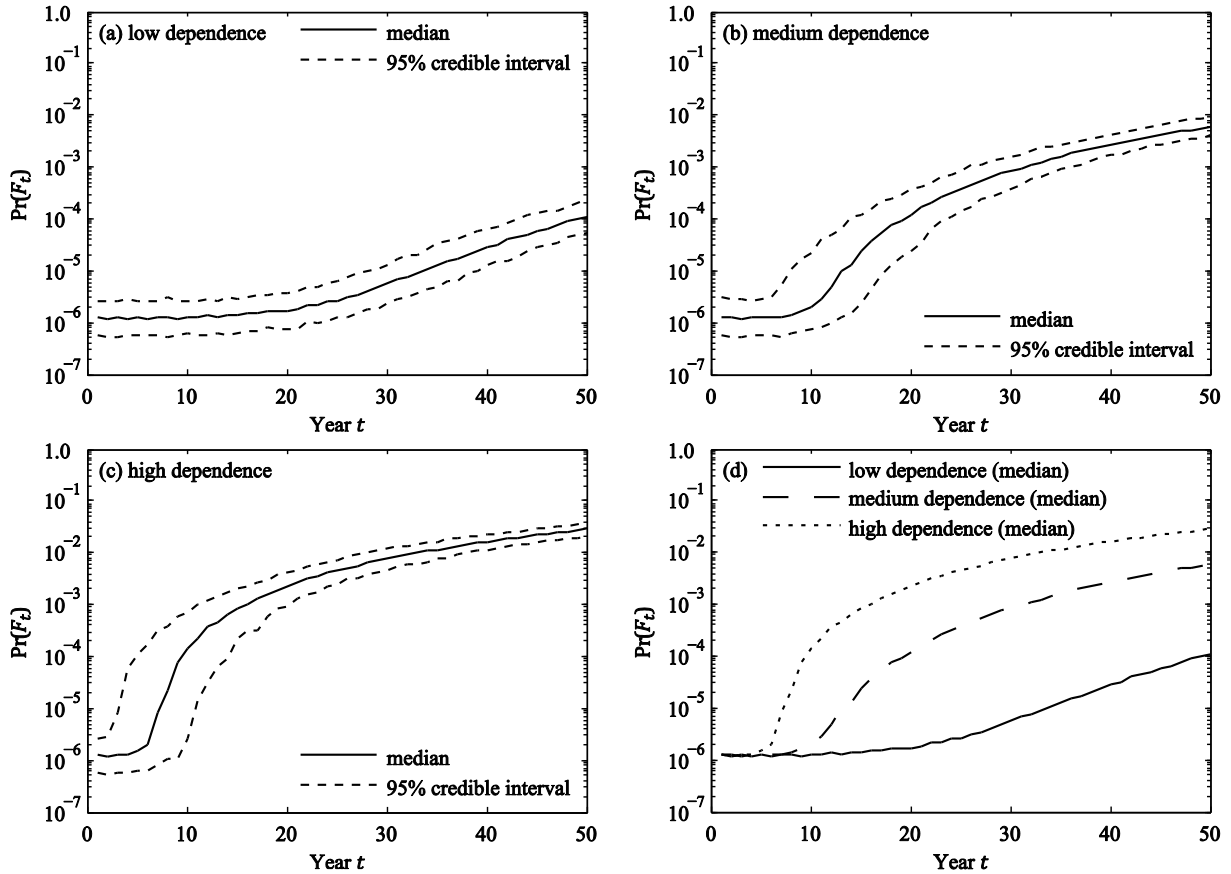
Figure 9. Median and 95% credible interval of the prior annual system failure probability $\Pr(F_t)$ of the Daniels system as a function of different degrees of dependence among hotspot fatigue behavior. Computations are performed with subset simulation as summarized in Section 4 with conditional probabilities $p_0 = 0.1$ and $N = 1000$ samples per subset level. (d) compares the respective medians of the prior annual system failure probability.

In general, a large dependence among element deterioration behavior increases the probability of joint occurrence of more than one element deterioration failures. Figure 9 shows that this behavior has a significant influence on the reliability of the Daniels system. This outcome is expected for a structural system with a large redundancy. In contrast, the results computed for the Zayas frame show that the influence of correlation among element deterioration failures is less pronounced for structural systems with limited or no redundancy (see Figure 2).

6.3 Posterior system reliability analysis

To study the effect of inspections on the reliability of the Daniels system, different inspection scenarios in terms of inspection times and coverage are considered. Each inspection is assumed to result in a no detection event. The same inspection model as presented in Section 5.3 is applied.

In the first scenario, hotspots {1 to 10} are inspected at time $t = 10$ years. The updated annual system failure probabilities $\Pr(F_t|Z_{0:t})$ of the Daniels system are shown in Figure 10 for each degree of dependence among hotspot fatigue behavior. In all three dependence cases, the system

failure probability decreases after the inspection due to the positive inspection outcome. After the inspection, the system failure probability is reduced to its lower limit, which corresponds to the reliability of the undamaged structure at the beginning of its service live. The subsequent increase in the annual system failure probability is most pronounced in the high-dependence case.
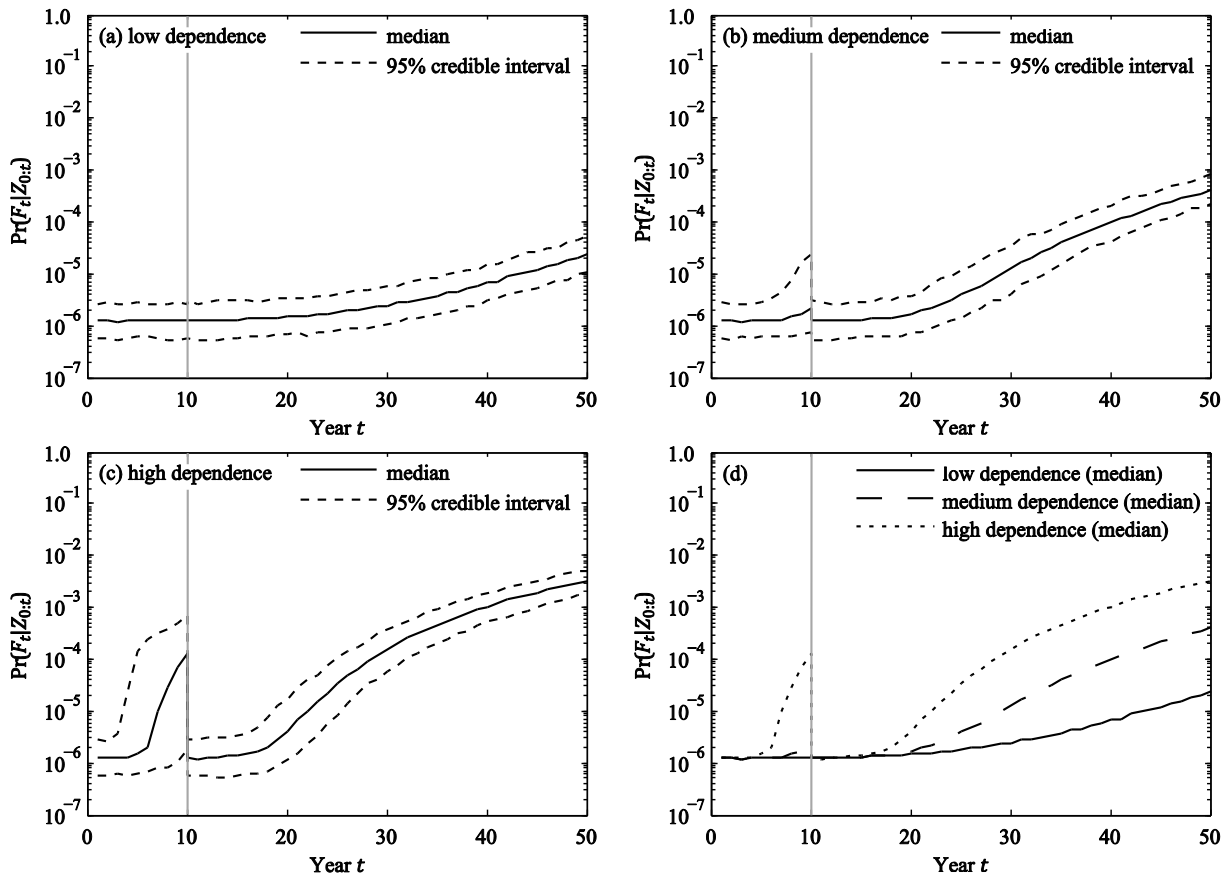
Figure 10. Median and 95% credible interval of the posterior annual system failure probability $\Pr(F_t|Z_{0:t})$ of the Daniels system as a function of different degrees of dependence among hotspot fatigue behavior. hotspots {1 to 10} are inspected in year 10. No fatigue cracks are detected. Computations are performed with subset simulation as summarized in Section 4 with conditional probabilities $p_0 = 0.1$ and $N = 1000$ samples per subset level. (d) compares the respective medians of the posterior annual system failure probability.

In the second scenario, different sets of hotspots are inspected at 10 year intervals. The inspection strategy is as follows: hotspots {1 to 10} are inspected at time $t = 10$ years, hotspots {11 to 20} are inspected at time $t = 20$ years, hotspots {21 to 30} are inspected at time $t = 30$ years and hotspots {31 to 40} are inspected at time $t = 40$ years. The results are shown in Figure 11. In all three dependence cases, the posterior annual system failure probability is close the annual failure probability of the undamaged structures after all inspections are performed.
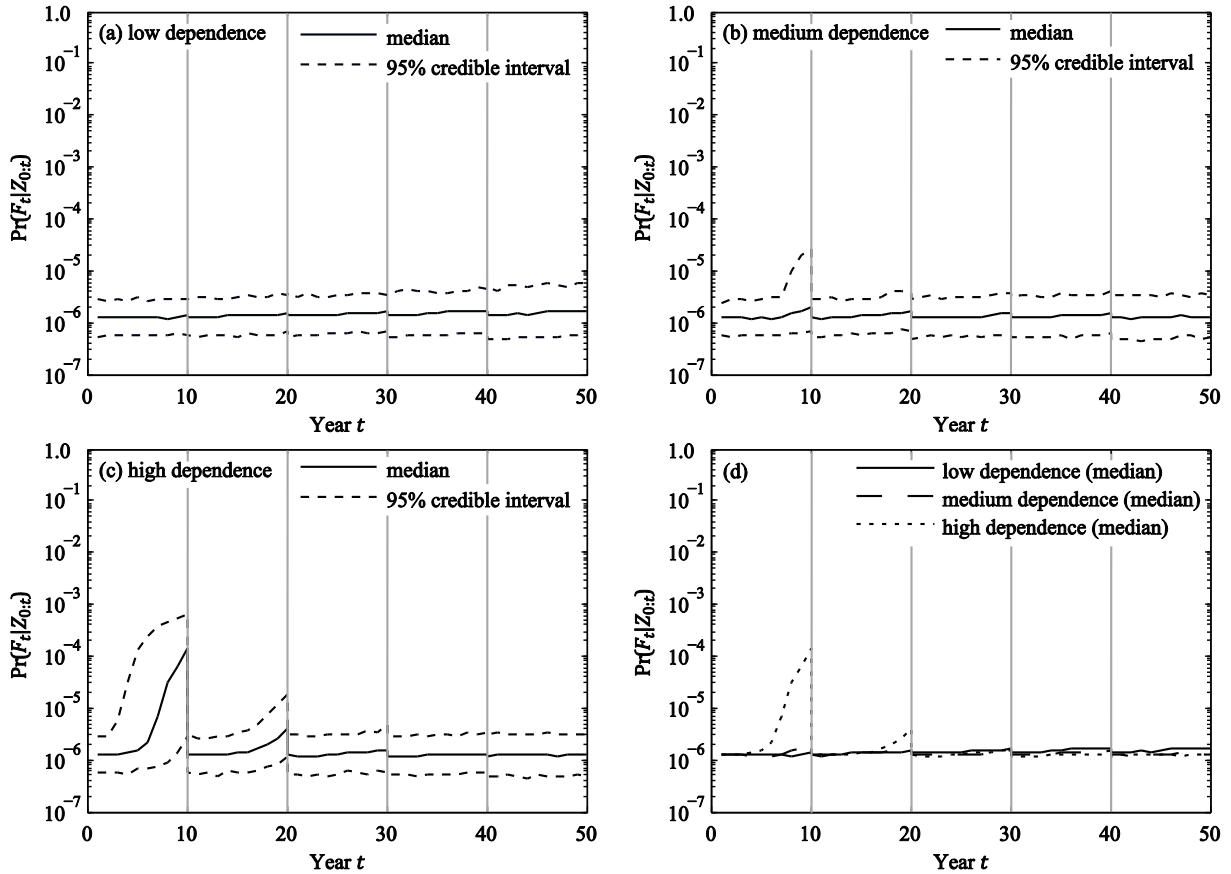
Figure 11. Median and 95% credible interval of the posterior annual system failure probability $\Pr(F_t|Z_{0:t})$ of the Daniels system as a function of different degrees of dependence among hotspot fatigue behavior. Hotspots {1 to 10} are inspected at time $t = 10$ years, hotspots {11 to 20} are inspected at time $t = 20$ years, hotspots {21 to 30} are inspected at time $t = 30$ years and hotspots {31 to 40} are inspected at time 40 years. Each inspection results in a no-detection event. Computations are performed with subset simulation as summarized in Section 4 with conditional probabilities $p_0 = 0.1$ and $N = 1000$ samples per subset level. (d) compares the respective medians of the posterior annual system failure probability.

7 Discussion

We propose a modeling and computational framework for analyzing the reliability of deteriorating structural systems and updating it with inspection and monitoring data. It enables an integral assessment of deterioration at the element level together with the structural system performance and structural condition information. The interdependences among the element deterioration states are included. Only few previous works have addressed such an integral system analysis (e.g. Lee and Song 2014; Schneider et al. 2015; Luque and Straub 2016). In contrast to these approaches, the main advantage of the proposed framework is the fact that it can be implemented easily through the use of subset simulation. It is computationally robust since it provides reasonably accurate solutions without a need for tailoring the algorithm to specific applications. It is also computationally efficient for many applications, as discussed further below.

800   The results in the paper demonstrate the importance of considering dependence among element
801   deterioration when evaluating the structural system reliability. For the considered redundant
802   systems, the dependence leads to a decrease in the prior (unconditional) system reliability. This
803   effect is more pronounced as the system redundancy increases (from the Zayas frame to the Daniels
804   system). When including inspection results, dependence among element deterioration means that
805   the state of non-inspected elements can be inferred from the inspection results. As long as
806   inspections do not indicate serious problems, this additional learning leads to a reduction of
807   uncertainty and hence to an increase in the overall system reliability. In the considered case studies,
808   the posterior (conditional) reliability after the inspections is fairly similar for the different degrees
809   of dependence. However, this is not expected to occur if inspections do indicate larger damage.

810   The framework can handle any type of information on the deterioration state of the structure, as
811   long as a corresponding likelihood function is formulated. In particular, the framework can also
812   include information from monitoring systems. For monitoring systems, which provide potentially
813   large amount of data, it might be beneficial to pre-process the data. In such a pre-processing step
814   (e.g. a system identification), the probability of the observed data given the deterioration states of
815   the structure is determined. This probability is the likelihood function that is inputted into
816   Equations (34) and (35). Such an approach is similar to a two-stage Bayesian analysis for system
817   identification (see Au and Zhang 2015).

818   The use of subset simulation is computationally rather efficient, as demonstrated in the case
819   studies. Here, no attempt was made to optimize the efficiency of subset simulation. The number
820   of samples per subset level was chosen such that the results have a reasonable accuracy. Their
821   accuracies can always be improved or reduced by increasing or decreasing the number of samples
822   per subset level. It should be noted, however, that the number of required subsets increases with
823   increasing amount of information, i.e. with decreasing $\Pr(Z_{e,0:t})$.

824   The proposed framework relies on the separation of the computation of the system deterioration
825   state $\mathbf{D}_t$ and structural system reliability conditional on $\mathbf{D}_t = \mathbf{d}_t$. Here, two situations must be
826   distinguished: Applications, in which the conditional probability $\Pr(F_t|\mathbf{D}_t = \mathbf{d}_t)$ can be pre-
827   computed, and those in which it cannot. The former occurs if the numbers of distinct states in $\mathbf{D}_t$
828   is limited. If the structural system reliability analysis is demanding, it might take some computation
829   time for establishing a database with all values of $\Pr(F_t|\mathbf{D}_t = \mathbf{d}_t)$, but this is typically not critical,
830   as this computation must be carried out only once and the database can be used for all subsequent
831   reliability updating calculations. If the number of states in $\mathbf{D}_t$ is too large to enable pre-
832   computation, because there are too many elements or because continuous damage states are
833   considered, $\Pr(F_t|\mathbf{D}_t = \mathbf{d}_t)$ must be computed on the fly. If such calculations are inexpensive (e.g.
834   through a FORM analysis), the separation of the system deterioration state and structural system
835   reliability is still computationally beneficial. In cases where pre-computation of $\Pr(F_t|\mathbf{D}_t = \mathbf{d}_t)$
836   is not an option, and in which it is expensive to compute it on the fly, there are two possible
837   strategies: (a) One can investigate the possibility of developing a response surface for

838   $\Pr(F_t | \mathbf{D}_t = \mathbf{d}_t)$. Since $\mathbf{D}_t$ is typically discrete, many of the classical response surface techniques

839   used in structural reliability will not be suitable. This is an area of future research. (b) Alternatively,

840   the proposed framework can be modified to solve the system deterioration updating and the system

841   reliability jointly. In this case, however, the advantages of the de-coupling are lost.

842   Potentials for further developments are seen in integrating the presented method into the

843   framework of pre-posterior decision analysis to identify optimal inspection, monitoring and

844   maintenance strategies for engineering structures (e.g. Straub and Faber 2005; Thöns and Faber

845   2013; Straub 2014).

8   Conclusions

847   We propose a novel approach to modeling and analyzing the system reliability of deteriorating

848   structural systems in conjunction with structural condition information, which considers stochastic

849   interdependence among the deterioration states of the structural elements. The approach provides

850   the means to consistently utilize inspection and monitoring information on the deterioration state

851   of structures to update the system failure probability. Through the application of subset simulation,

852   the approach can be implemented relatively easily and is considerably more efficient than crude

853   Monte Carlo simulation.

854

859

References

861   Altamura, A. and D. Straub (2014). "Reliability assessment of high cycle fatigue under variable
862   amplitude loading: review and solutions." Engineering Fracture Mechanics **121**: 40-66.

863   Au, S.-K. and J. L. Beck (2001). "Estimation of small failure probabilities in high dimensions by
864   subset simulation." Probabilistic Engineering Mechanics **16**(4): 263-277.

865   Au, S.-K., F. A. DiazDelaO and I. Yoshida (2015). "Bayesian updating and model class selection
866   with Subset Simulation." eprint arXiv:1510.06989.

867   Au, S.-K. and F.-L. Zhang (2015). "Fundamental two-stage formulation for Bayesian system
868   identification, Part I: General theory." Mechanical Systems and Signal Processing.

869   Betz, W., I. Papaioannou and D. Straub (2014a). "Numerical methods for the discretization of
870   random fields by means of the Karhunen–Loève expansion." Computer Methods in
871   Applied Mechanics and Engineering **271**: 109–129.

872   Betz, W., I. Papaioannou and D. Straub (2014b). Adaptive variant of the BUS approach to Bayesian
873   updating. 9th International Conference on Structural Dynamics (EURODYN 2014). Porto,
874   Portugal.

Ciampoli, M. (1998). "Time dependent reliability of structural systems subject to deterioration." Computers & Structures **67**(1–3): 29-35.

Daniels, H. E. (1945). "The statistical theory of the strength of bundles of threads. I." Proceedings of the Royal Society of London: 405-435.

Ditlevsen, O. and P. Bjerager (1986). "Methods of structural systems reliability." Structural Safety **3**(3): 195-229.

Ditlevsen, O. and H. O. Madsen (1996). Structural Reliability Methods, John Wiley & Sons Ltd.

Enright, M. P. and D. M. Frangopol (1999). "Condition prediction of deteriorating concrete bridges using Bayesian updating." Journal of Structural Engineering **125**(10): 1118-1125.

Estes, A. and D. Frangopol (1999). "Repair Optimization of Highway Bridges Using System Reliability Approach." Journal of Structural Engineering **125**(7): 766-775.

Faber, M. H., S. Engelund, J. D. Sørensen and A. Bloch (2000). Simplified and Generic Risk Based Inspection Planning. 19th Conference on Offshore Mechanics and Arctic Engineering (OMAE), New Orleans, Louisiana, USA.

Faber, M. H., D. Straub and M. A. Maes (2006). "A computational framework for risk assessment of RC structures using indicators." Computer-Aided Civil and Infrastructure Engineering **21**(3): 216-230.

Fricke, W. (2003). "Fatigue analysis of welded joints: state of development." Marine Structures **16**(3): 185-200.

Gollwitzer, S. and R. Rackwitz (1990). "On the reliability of Daniels systems." Structural Safety **7**(2-4): 229–243.

Gurney, T. R. (1978). An analysis of some recent fatigue crack propagation data for steels subjected to pulsating tension loading. Report 1978E, The Welding Institute TWI, UK

Hergenröder, M. (1992). Zur statistischen Instandhaltungsplanung für bestehende Betonbauwerke bei Karbonatisierung des Betons und möglicher Korrosion der Bewehrung PhD, Technische Universität München.

Hohenbichler, M. and R. Rackwitz (1981). "Non-Normal Dependent Vectors in Structural Safety." Journal of the Engineering Mechanics Division **107**(6): 1227-1238.

Hohenbichler, M. and R. Rackwitz (1983). "First-order concepts in system reliability." Structural Safety **1**(3): 177-188.

Lee, Y.-J. and J. Song (2014). "System Reliability Updating of Fatigue-Induced Sequential Failures." Journal of Structural Engineering **140**(3).

Li, C. Q. (1995). "Computation of the failure probability of deteriorating structural systems." Computers & Structures **56**(6): 1073-1079.

Li, Q., C. Wang and B. R. Ellingwood (2015). "Time-dependent reliability of aging structures in the presence of non-stationary loads and degradation." Structural Safety **52, Part A**: 132-141.

Li, Y., T. Vrouwenvelder, G. H. Wijnants and J. Walraven (2004). "Spatial variability of concrete deterioration and repair strategies." Structural Concrete **5**(3): 121-129.

Lin, Y. K. and J. N. Yang (1985). "A stochastic theory of fatigue crack propagation." AIAA Journal **23**(1): 117-124.

Liu, P.-L. and A. Der Kiureghian (1986). "Multivariate distribution models with prescribed marginals and covariances." Probabilistic Engineering Mechanics **1**(2): 105-112.

Luque, J., R. Hamann and D. Straub (2016). "Spatial probabilistic modeling of corrosion in ships structures." ASCE-ASME Journal of Risk and Uncertainty in Engineering Systems, Part B: Mechanical Engineering: submitted.

Luque, J. and D. Straub (2016). "Reliability analysis and updating of deteriorating systems with dynamic Bayesian networks." Structural Safety **62**: 34-46.

Madsen, H. O. (1987). Model updating in reliability theory. <u>5th International Conference on Applications of Statistics and Probability in Civil Engineering (ICASP 5)</u>. Vancouver, Canada.

Madsen, H. O. (1997). Stochastic modeling of fatigue crack growth and inspection. <u>Probabilistic Methods for Structural Design</u>. C. Guedes Soares, Kluwer Accademic Publishers, Netherlands.

Madsen, H. O., S. Krenk and N. C. Lind (1986). <u>Methods of Structural Safety</u>, Prentice Hall.

Maes, M. A. and M. Dann (2007). "Hierarchical Bayes methods for systems with spatially varying condition states." <u>Canadian Journal of Civil Engineering</u> **34**(10): 1289-1298.

Malioka, V. (2009). <u>Condition Indicators for the Assessment of Local and Spatial Deterioration of Concrete Structures</u>. PhD, ETH Zurich.

Maljaars, J. and A. C. W. M. Vrouwenvelder (2014). "Probabilistic fatigue life updating accounting for inspections of multiple critical locations." <u>International Journal of Fatigue</u> **68**: 24-37.

Melchers, R. E. (1999a). "Corrosion uncertainty modelling for steel structures." <u>Journal of Constructional Steel Research</u> **52**(1): 3-19.

Melchers, R. E. (1999b). <u>Structural Reliability Analysis and Prediction</u>, John Wiley and Sons Ltd.

Moan, T. (2005). "Reliability-based management of inspection, maintenance and repair of offshore structures." <u>Structure and Infrastructure Engineering</u> **1**(1): 33-62.

Moan, T. and R. Song (2000). "Implications of Inspection Updating on System Fatigue Reliability of Offshore Structures." <u>Journal of Offshore Mechanics and Arctic Engineering</u> **122**(3): 173-180.

Moan, T., O. T. Vardal, N. C. Hellevig and K. Skjoldli (2000). "Initial crack depth and PoD values inferred from in-service observations of cracks in North Sea jackets." <u>Journal of Offshore Mechanics and Arctic Engineering</u> **122**: 157-162.

Mori, Y. and B. Ellingwood (1993). "Reliability-Based Service-Life Assessment of Aging Concrete Structures." <u>Journal of Structural Engineering</u> **119**(5): 1600-1621.

Naess, A., B. J. Leira and O. Batsevych (2009). "System reliability analysis by enhanced Monte Carlo simulation." <u>Structural Safety</u> **31**(5): 349-355.

Papaioannou, I., W. Betz, K. Zwirgelmaier and D. Straub (2015). "MCMC Algorithms for Subset Simulation." <u>Probabilistic Engineering Mechanics</u> **41**: 89-103.

Paris, P. C. and F. A. Erdogan (1963). "A critical analysis of crack propagation laws." <u>Journal of Basic Engineering</u> **85**: 528-534.

Qin, J. and M. H. Faber (2012). "Risk Management of Large RC Structures within a Spatial Information System." <u>Computer-Aided Civil and Infrastructure Engineering</u> **27**: 385–405.

Schneider, R., J. Fischer, M. Bügler, M. Nowak, S. Thöns, A. Borrmann and D. Straub (2015). "Assessing and updating the reliability of concrete bridges subjected to spatial deterioration - principles and software implementation." <u>Structural Concrete</u> **16**(3): 356–365.

Schneider, R., S. Thöns, W. Rücker and D. Straub (2013). Effect of different inspection strategies on the reliability of Daniels systems subjected to fatigue. <u>11th International Conference on Structural Safety & Reliability (ICOSSAR 2013)</u>. New York, USA.

Schuëller, G. I. and H. J. Pradlwarter (2007). "Benchmark study on reliability estimation in higher dimensions of structural systems – An overview." <u>Structural Safety</u> **29**(3): 167-182.

Skallerud, B. and J. Amdahl (2002). <u>Nonlinear analysis of offshore structures</u>. UK, Reasearch Studies Press Ltd.

Song, J. and W.-H. Kang (2009). "System reliability and sensitivity under statistical dependence by matrix-based system reliability method." <u>Structural Safety</u> **31**(2): 148–156.

Stewart, M. and D. Val (1999). "Role of Load History in Reliability-Based Decision Analysis of Aging Bridges." <u>Journal of Structural Engineering</u> **125**(7): 776-783.

Stewart, M. G. and J. A. Mullard (2007). "Spatial time-dependent reliability analysis of corrosion damage and the timing of first repair for RC structures." Engineering Structures **29**(7): 1457-1464.

Straub, D. (2004). Generic Approaches to Risk Based Inspection Planning for Steel Structures, ETH Zürich.

Straub, D. (2011a). "Reliability updating with equality information." Probabilistic Engineering Mechanics **26**(2): 254–258.

Straub, D. (2011b). Reliability updating with inspection and monitoring data in deteriorating reinforced concrete slabs. 11th International Conference on Applications of Statistics and Probability in Civil Engineering. Zurich, Switzerland.

Straub, D. (2014). "Value of Information Analysis with Structural Reliability Methods." Structural Safety **49**: 75-85.

Straub, D. and A. Der Kiureghian (2010). "Bayesian network enhanced with structural reliability methods: Methodology." Journal of Engineering Mechanics **136**(10): 1248-1258.

Straub, D. and A. Der Kiureghian (2011). "Reliability acceptance criteria for deteriorating elements of structural systems." Journal of Structural Engineering **137**(12): 1573-1582.

Straub, D. and M. H. Faber (2003). Modeling Dependency in Inspection Performance. 9th International Conference on Applications of Statistics and Probability in Civil Engineering. San Francisco, California.

Straub, D. and M. H. Faber (2005). "Risk based inspection planning for structural systems." Structural Safety **27**: 335–355.

Straub, D. and M. H. Faber (2007). "Temporal Variability in Corrosion Modeling and Reliability Updating." Journal of Offshore Mechanics and Arctic Engineering **129**(4): 265-272.

Straub, D. and I. Papaioannou (2015a). Bayesian analysis for learning and updating geotechnical parameters and models with measurements. Risk and reliability in geotechnical engineering. K.-K. Phoon and J. Ching, CRC Press.

Straub, D. and I. Papaioannou (2015b). "Bayesian updating with structural reliability methods." Journal of Engineering Mechanics **141**(3).

Straub, D., I. Papaioannou and W. Betz (2016). "Bayesian analysis of rare events." Journal of Computational Physics: accepted.

Tang, W. H. (1973). "Probabilistic updating of flaw information." Journal of Testing and Evaluation **1**(6): 459-467.

Thoft-Christensen, P. and Y. Murotsu (1986). Application of Structural Systems Reliability Theory, Springer-Verlag.

Thoft-Christensen, P. and J. D. Sørensen (1987). "Optimal strategy for inspection and repair of structural systems." Civil Engineering Systems **4**: 94-100.

Thöns, S. and M. H. Faber (2013). Assessing the Value of Structural Health Monitoring. 11th International Conference on Structural Safety & Reliability (ICOSSAR 2013). New York, USA.

Ultiguide (1999). Best practice guidelines for use of non-linear methods in documentation of ultimate limit states for jacket type offshore structures, Det Norske Veritas (DNV), Norway

USFOS (2014). Ultimate Strength of Framed Offshore Structures. Version 8-7, USFOS A/S, Norway

Vrouwenvelder, A. C. W. M. (2004). Spatial correlation aspects in deterioration models. 2nd International Conference on Lifetime-Oriented Design Concepts. Bochum, Germany.

Wen, Y. K. and H.-C. Chen (1987). "On fast integration for time variant structural reliability." Probabilistic Engineering Mechanics **2**(3): 156-162.

1018   Zayas, V. A., S. A. Mahin and E. P. Popov (1980). Cyclic inelastic behavior of steel offshore
1019   structures. UCB/EERC-80/27, University of California, Berkley, USA

1020